Prepared for the National Aeronautics and Space Administration

Geologic Map of MTM –30247, –35247, and –40247 Quadrangles, Reull Vallis Region of Mars

By Scott C. Mest and David A. Crown

Pamphlet to accompany

Scientific Investigations Map 3245

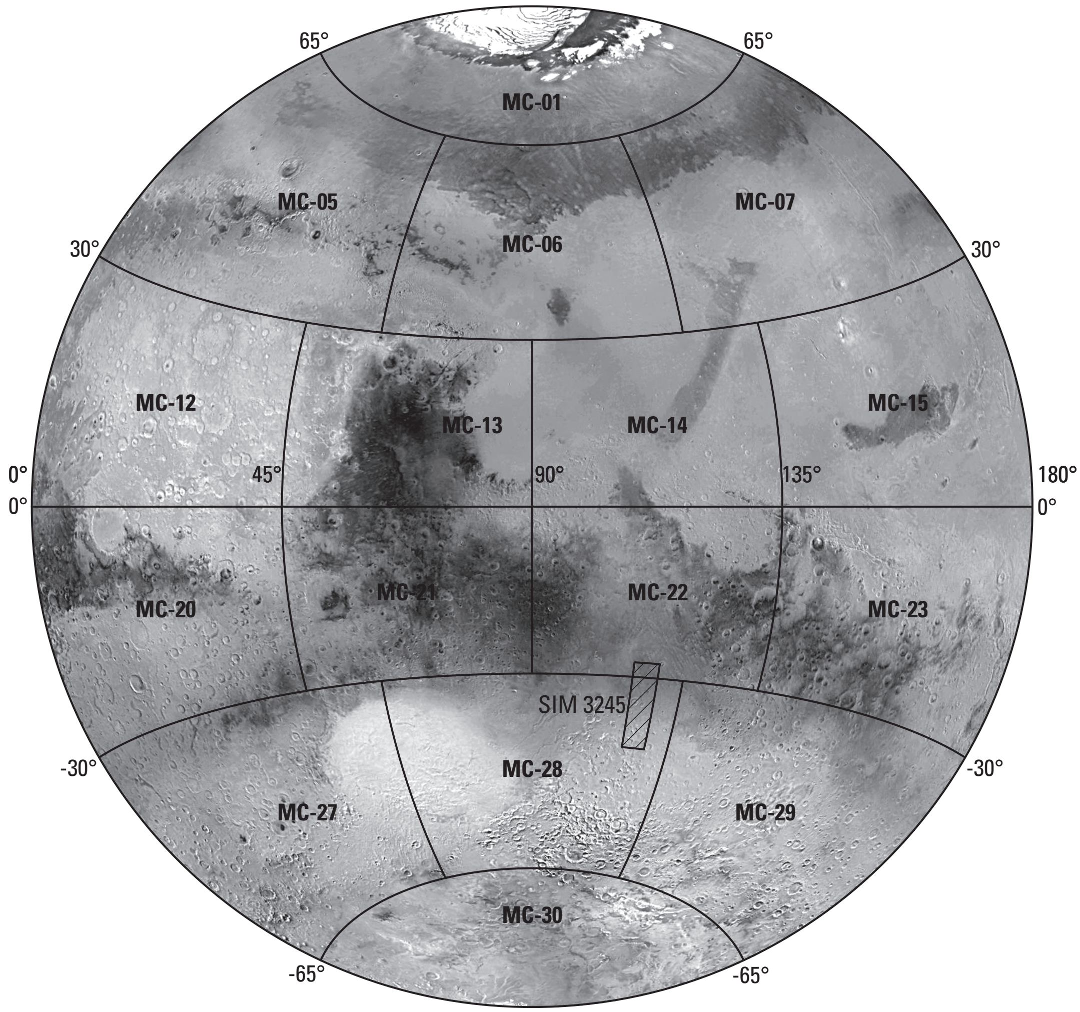

2014

U.S. Department of the Interior

U.S. Geological Survey

Contents

Introduction....1
Physiographic Setting....1
Data 2
Contact Types....2
Fluvial Features....2
    Waikato Vallis....3
    Eridania Planitia....4
    Reull Vallis....4
    Channels....5
    Gullies 5
Structural Features....5
Crater Counting Methodology....6
Stratigraphy....6
    Highland Materials....6
    Plains Materials....6
    Vallis Materials....9
Surficial Deposits....11
    Crater Materials....12
Geologic History....14
Acknowledgments....15
References Cited....15

Tables

1. Crater size-frequency data and time-stratigraphic determinations for Reull Vallis region of Mars....19
2. Contact relations of geologic units in Reull Vallis region of Mars....20

Introduction

Mars Transverse Mercator (MTM) –30247, –35247, and –40247 quadrangles cover a portion of southern Hesperia Planum and the highlands of eastern Promethei Terra, east of the Hellas basin (fig. 1). The map area (lat 27.5–42.5° S., long 110–115° E.) consists of cratered ancient highland materials of moderate relief, isolated knobs and massifs of rugged mountainous materials, extensive tracts of plains, and surficial deposits. Waikato and Reull Valles extend through plains and highland terrains. Regional slopes are generally to the southwest toward the Hellas basin (fig. 1), but local slopes (for example, highlands to plains) dominate the landscape.

The Martian highlands cover more than 60 percent of the planet's surface and are primarily found in the southern hemisphere (Tanaka and others, 1992). Most of the highlands consist of rugged, densely cratered terrains believed to represent the final phase of heavy bombardment in the inner solar system ~4.0 billion years ago (Murray and others, 1971; Schubert and others, 1992; Tanaka and others, 1992). Parts of the Martian highlands show evidence of extensive degradation and modification. The map area exhibits landforms created by numerous geologic processes, including tectonism, fluvial activity, and mass wasting. The occurrence of features that may have been formed or modified by water, such as the eastern Hellas valles and valley networks, has significant implications for past Martian conditions. Determining the geology of the highlands east of the Hellas basin provides a better understanding of the role and timing of volatile-driven activity in the evolution of the highlands.

Geologic mapping at 1:1,000,000 scale from analysis of images—including Mars Observer (MO) Thermal Emission Imaging System (THEMIS) daytime infrared (IR) and visible (VIS), Mars Reconnaissance Orbiter (MRO) High Resolution Imaging Science Experiment (HiRISE) and Context Camera (CTX), Mars Global Surveyor (MGS) Mars Orbiter Camera (MOC), and Viking Orbiter (VO) images—and MGS Mars Orbiter Laser Altimeter (MOLA) topographic data complements previous local and regional geologic mapping and geomorphic studies of Reull Vallis (Mest and Crown, 2001, 2002, 2003) and the other eastern Hellas valles (Crown and others, 1992; Price, 1998), drainage networks (Mest and Crown, 2001, 2004; Ivanov and others, 2005; Mest and others, 2010), and highland debris aprons (Pierce and Crown, 2003). Crater size-frequency distributions have been compiled to constrain the relative ages of geologic units and determine the timing and extents of the observed geologic processes.

Physiographic Setting

Noachian materials are the principal components of the rugged highlands surrounding the Hellas basin and represent the oldest rocks on Mars (Murray and others, 1971; Tanaka, 1986; Tanaka and others, 1988, 1992; Schubert and others, 1992). Within the circum-Hellas region, erosion of highland materials began during the Late Noachian Epoch and continued throughout the Hesperian Period, resulting in deposition of extensive plains materials in and around the Hellas basin. Regionally, the units of the Hellas basin and its surrounding rim are grouped into the Hellas assemblage and range from the ancient basin-rim unit, consisting of rugged highland plateaus and massifs dissected by channels and valley networks, to younger plains units, some of which contain channels, ridges, scarps, and mesas (for example, Greeley and Guest, 1987; Crown and others, 1992; Tanaka and Leonard, 1995; Mest and Crown, 2001; Tanaka and others, 2002).

Highland volcanism began north and northwest of the map area in the Late Noachian/Early Hesperian Epochs with the formation of Tyrrhenus and Hadriacus Paterae (Crown and others, 1992; Tanaka and Leonard, 1995; Crown and Greeley, 1993, 2007; Gregg and others, 1998), initially by explosive eruptions (Greeley and Spudis, 1981; Greeley and Crown, 1990; Crown and Greeley, 1993), and ending with effusive activity during the middle to Late Hesperian/Early Amazonian (Crown and others, 1992; Mest and Crown, 2001). The ridged plains of Hesperia Planum (Tanaka, 1986; Greeley and Guest, 1987), the basal referent for the Hesperian System, is one of many areally extensive plains-forming units found on the surface of Mars (Scott and Tanaka, 1986; Greeley and Guest, 1987) believed to have been emplaced as flood lavas (Potter, 1976; King, 1978; Greeley and Spudis, 1981; Scott and Tanaka, 1986; Greeley and Guest, 1987). However, despite the abundance of high-resolution images from recent missions (MOC, THEMIS, CTX, and HiRISE), definitive evidence for the presence of volcanic features (edifices, flow fronts, rilles) has not been observed, and thus a volcanic origin of these plains is uncertain (Mest and Crown, 2001; Crown and others, 2005, 2007; Gregg and Crown, 2005, 2007).

The abundance of channels and valley networks in the eastern Hellas region, along with the presence of several canyon systems, suggest water played a major role in modifying this part of the Martian landscape. Well-developed valley networks appear to be the oldest fluvial features in the area; they are found in rugged ancient highland terrains and are most likely Noachian to Hesperian in age (Crown and Mest, 1997; Mest and Crown, 2001, 2002, 2003). The presence of widespread plains units northeast of the Hellas basin provides evidence that extensive degradation and resurfacing occurred in the highlands. Subsequent erosion of these plains units is believed to have occurred in the Late Hesperian/Early Amazonian Epochs (Greeley and Guest, 1987).

Activity along the highland valles (Waikato, Reull, Dao, Niger, and Harmakhis) occurred primarily during the Hesperian Period, with some activity extending into the Amazonian. Recent studies of these canyon systems suggest an origin by subsurface flow and collapse of volatile-rich plains materials combined with erosion by fluvial processes, followed by modification by wall retreat (Crown and others, 1992, 2005;

Tanaka and Leonard, 1995; Crown and Mest, 1997; Mest and Crown, 2001, 2002, 2003). Most of the valles head within or are adjacent to a major local volcanic feature: Dao Vallis cuts into the flank materials of Hadriacus Mons; Niger and Harmakhis Valles are located adjacent to the Tyrrhenus Mons lava flow field; Waikato Vallis is located in the ridged plains of Hesperia Planum; and Reull Vallis begins at the western edge of the depression of Eridania Planitia (figs. 1, 2). The fact that these canyons are in close proximity to volcanic features suggests channel formation may be in part due to mobilization and release of subsurface volatiles by volcanic heat (Squyres and others, 1987; Crown and others, 1992).

Lastly, evidence of mass wasting in the highlands east of Hellas basin has been observed in the form of debris aprons and flows that extend from highland massifs, interior crater walls, and valles walls and appear to be the youngest features observed (Crown and others, 1992, 1997, 2005; Crown and Stewart, 1995; Tanaka and Leonard, 1995; Crown and Mest, 1997; Mest and Crown, 2001; Pierce and Crown, 2003).

The history of volatiles within Hesperia Planum and the surrounding highlands has been analyzed in broad-scale regional studies (Maxwell and Craddock, 1995; Crown and others, 2005; Mest and others, 2010), and some general consensus has emerged on the timing and sources of volatiles within the eastern Hellas/Hesperia Planum regions. Studies have suggested that hydrologic activity in this area began in the Noachian with fluvial dissection of the adjacent highlands (Mest and others, 2010). Ivanov and others (2005) suggested that water accumulated within a pre-ridged plains depression in the location of the present-day Hesperia Planum. According to Ivanov and others (2005), this volatile reservoir was later depleted (1) in the Early Hesperian by erosion prior to emplacement of the ridged plains, (2) in the Late Hesperian with formation of the eastern Hellas valles (Crown and others, 1992, 2005; Mest and Crown, 2001), and (3) in the Early Amazonian by formation of lobate debris aprons (Pierce and Crown, 2003) and viscous flow features (Berman and others, 2009) in the highlands of Promethei Terra. Mid-latitude mantling deposits, now observed in various stages of degradation (Mustard and others, 2001), cover most surfaces in the southern part of the map area and are a recent source of volatiles to the region that may be directly related to the youngest fluvial and glacial landforms east of Hellas basin.

Data

Several data sets were used to map MTM –30247, –35247, and –40247 quadrangles. A THEMIS daytime IR mosaic (~230 m/pixel) was used as the base for displaying the map. THEMIS VIS (17–19 m/pixel), CTX (~5.1 m/pixel), and MOC narrow angle (1.5–8 m/pixel) images were provided by the U.S. Geological Survey (USGS) and, in addition to the THEMIS daytime IR mosaic, were used to identify contacts and features (craters, valleys, structures), to assist in characterizing geologic materials, and to measure the diameters of craters. A MOLA digital elevation model (DEM), with a resolution of 128 pixels/degree, was used to evaluate the overall topography of the map area and assess the distribution of units and features within the map area with respect to their relative elevations.

Contact Types

This mapping effort uses standard contact types defined by the USGS, including certain, approximate, and inferred contacts. A "certain" contact type indicates a clear delineation of material units based on appearance and (or) relative age. Most units in the map area are delineated by a certain contact. An "approximate" contact type indicates certainty of the existence of the contact but uncertainty in the location of the contact due to data quality and (or) modification of the surface to obscure its precise location. For example, we use approximate contacts to delineate older impact crater ejecta deposits, such as Dowa/Pál ejecta materials, that do not display sharp contrasts with underlying plains due to the thinning of the distal parts of the deposit, as well as subsequent modification (erosion, mobilization, and deposition) of ejecta and plains materials by fluvial and eolian processes. Lastly, we use an "inferred" contact type in a handful of instances to delineate units that are similar in appearance and may be of similar origin but have clearly been modified differently. For example, inferred contacts are used to delineate highly degraded crater materials from highlands materials (mountainous material and basin rim unit), where a crater rim clearly identifies the presence of an impact crater, but the topography is too subtle and surface characteristics are too similar to the adjacent highland materials to support usage of another contact type.

Fluvial Features

Fluvial processes appear to have played a major role in the geologic evolution of the map area. Numerous valley networks, single channels, and gullies are incised within many of the geologic units, including the ridged and modified ridged plains, smooth plains (upper and lower members), etched and mottled plains, upper Reull Vallis floor material, and materials associated with impact craters. Furthermore, the presence of Waikato and Reull Valles indicate that significant amounts of material were eroded and transported from Hesperia Planum and Promethei Terra.

Waikato Vallis

Waikato Vallis[1] (fig. 2) extends ~400 km through the plains of Hesperia Planum and is believed to be the source area for at least some of the fluids that carved Reull Vallis (Mest and Crown, 2001; Ivanov and others, 2005; Kostama and others, 2007). The first expression of Waikato Vallis occurs as a shallow (150–200 m deep) elongated depression in the north-central part of the map area that extends for ~140 km before transitioning to the main canyon system. The north boundary of the depression is gradual (slope ~0.5°), whereas the east and west boundaries appear as distinct low-relief scarps and (or) coincide with wrinkle ridges. The northernmost part of the depression is widest at ~47 km across, then narrows to ~24 km, where the depression intersects a fairly pristine wrinkle ridge and remains relatively consistent in width until it opens into the main canyon.

Two narrow channels are incised within the northern and southern parts of this depression for nearly its entire length (fig. 3*A*). The northern channel originates within a broad, flat-lying, scarp-bounded area of the ridged plains where several small channels, low-relief scarps, and a streamlined teardrop-shaped island converge. This northern channel is sinuous, ~500–800 m wide and ~2–5 m deep, and at several locations along its length the channel is braided (fig. 3*B*). These braided areas all occur on the north side of low-relief wrinkle ridges that cross-cut the channel, suggesting water within the channel may have ponded behind the ridges until it eroded through the ridges and became confined within the channel again. This channel continues south for ~60 km before terminating in the ridged plains and transitioning into a (subtle) positive relief feature (fig. 3*C*). Secondary craters from craters Dowa and (or) Pál (located ~160 km to the west) are superposed on this northern channel. The secondary craters appear morphologically similar and relatively pristine in both the plains and the channel where they cross, indicating that the impact events of Dowa and (or) Pál likely postdate incision of this channel.

The southern channel originates at a theater-headed alcove and displays steep walls along most of its length (fig. 3*D*). This channel is as much as 55 m deep and 0.5–1.5 km wide and generally widens prior to crossing intersecting wrinkle ridges and narrows where it cuts through and south of the ridges. Similar to the northern channel, the ridges likely impeded flow until the ridges were breached, but, unlike the northern channel, ponding water resulted in widening of the channel and not braiding. Unlike the northern channel, the southern channel contains a narrow channel incised on its floor for short distances along its length. The southern channel terminates prior to intersecting the main canyon of Waikato Vallis, where the channel has been impacted by a 5.5-km-diameter crater (a in fig. 3*A*). The pre-crater course of the channel, however, can be traced in the ejecta and the north and southwest rim of the crater, suggesting minor amounts of fluvial activity may have occurred after this impact event.

The main canyon of Waikato Vallis originates at the southern end of the elongated depression and continues south for ~260 km toward Eridania Planitia (figs. 2, 4). Waikato Vallis consists of a series of 40- to 70-km-wide, near-circular, ~250-m-deep scarp-bounded depressions connected by a narrower (~4–15 km) canyon (Mest and others, 1998; Mest and Crown, 2001). Based on the high density of wrinkle ridge-rings throughout this part of Hesperia Planum, which are believed to reflect the locations of buried impact craters (Bryan, 1973; Chicarro and others, 1985), we presume that the near-circular depressions reflect impact craters that were buried by the ridged plains and exhumed during vallis formation. Waikato Vallis appears to have debauched into Eridania Planitia, where it terminates. Any visible connection between Waikato Vallis and Eridania Planitia is obscured by impact materials from craters Fiztroy, Avarua, Fancy, and Cayon, and a 34-km-diameter impact crater along the east edge of the map area (fig. 4*A*). However, MOLA data show that, despite the presence of this ejecta, it is likely water flowed to the east of Fancy and Cayon toward Eridania Planitia (fig. 2*B*). These two craters, as well as Fitzroy to the west and the 34-km-diameter crater to the east, provide important constraints on the timing of vallis formation. Fancy and Cayon contain knobs of mottled ridged plains material on their floors indicating both craters were inundated with ridged plains material; the remnant rims of two smaller craters to the east of Fancy and Cayon also appear to have been buried by plains materials, likely ridged plains material, but have subsequently been buried by smooth plains material and (or) ejecta. Following emplacement of ridged plains material, craters Fitzroy and Avarua formed and emplaced ejecta across this part of the plains. Waikato Vallis then formed, via a combination of subsidence and fluvial erosion, causing collapse of plains materials north of and within Fancy and Cayon and likely to the east of these craters. Water ponded within Fancy and Cayon and resulted in deposition of Waikato Vallis floor materials within these craters. The southwest rim of crater Fancy is breached; a small channel extends from this breach toward the smooth plains to the south (fig. 5), suggesting enough water was able to downcut the rim of Fancy and drain from the craters, thus eroding ejecta from Fitzroy and smooth plains material.

Grooves incised in Waikato Vallis floor materials in the northernmost part of the canyon (fig. 4*B*) and along the east edge of the depression just northeast of craters Fancy and Cayon (fig. 4*A*) suggest flow of water through the canyon eroded collapsed ridged and mottled ridged plains and Waikato Vallis floor materials. Inliers of ridged plains and modified ridged plains materials are found throughout Waikato Vallis and occur as streamlined islands and chaotic clusters of polygonal blocks. Ridges visible on the floor of Waikato Vallis have subdued morphologies and lack the characteristic broad rise and crenulated ridge crest observed in the ridges extending into the plains. This lack of primary wrinkle-ridge morphology,

[1]Mest and Crown (2001) defined three morphologically distinct segments for Reull Vallis, including Segment 1 (now Waikato Vallis) and Segments 2 and 3 (now upper and lower Reull Vallis, respectively).

combined with notches observed in the ridges, indicates fluvial erosion of the ridges resulting from the Waikato outflow event. This further suggests that we are observing ridge structures at depth and providing constraints on the relative timing of plains emplacement, ridge formation, and vallis formation.

The overall morphology of Waikato Vallis and features identified within and around the vallis suggest this system formed by a combination of surface flow of water and collapse of ridged plains material by removal of subsurface water (Mest and Crown, 2001). The elongated northern depression and chaotic clusters of blocks within the canyon suggest removal of subsurface water and collapse of plains material along zones of structural weakness coinciding with buried impact craters. Subsidence may have been largely responsible for the overall shape of Waikato Vallis. Sinuous channels in the northern depression and plains adjacent to the main canyon of Waikato Vallis, grooves on the vallis floor, and streamlined inliers of ridged plains material suggest surface flow was also important in shaping the system and removing material from the canyon via erosion.

Eridania Planitia

An obvious surface connection between Waikato Vallis and Reull Vallis is not apparent. Previous mapping, prior to accurate topographic data, suggested the two valles were once connected, but the connection was subsequently buried by younger plains or eroded (Mest and Crown, 2001). However, MOLA data show there is no obvious channel-form connection between the two systems; rather, water evacuated from Waikato Vallis may have been stored temporarily in the depression recently named Eridania Planitia[2] (Ivanov and others, 2005; Kostama and others, 2007).

Eridania Planitia (~3,100 km^2) is located south of Hesperia Planum (fig. 1; lat 33–44° S., long 111–133° E.). Relative to the surrounding terrain, Eridania Planitia lies ~1 km below the ridged plains to the north and ~2 km below the adjacent highlands. The plains throughout Eridania Planitia are cross-cut by numerous wrinkle ridges, but these ridges are more degraded than in the higher-standing ridged plains to the north, and they appear mantled in some areas, especially within the map area. In general, these low-lying plains would have acted as a depositional sink for fluvial sediments being eroded from the adjacent highlands, as shown by highland valley networks intersecting the plains along the western extent of Eridania Planitia (Ivanov and others, 2005). In addition, Eridania Planitia may have temporarily contained water evacuated from the ridged plains to the north via Waikato Vallis; crater Lipik (diameter, 56 km; lat 38.42° S., long 111.5° E.) and massifs within Promethei Terra may have acted as barriers that trapped water within Eridania Planitia (fig. 6). The materials covering Eridania Planitia, at least in the vicinity of the map area and possibly to the east, likely consist of sediments eroded from both the adjacent highlands and the ridged plains to the north (through Waikato Vallis) that have subsequently undergone eolian erosion, mapped in this study as etched plains materials (described below). This stored water was able to breach Lipik and highland massifs contributing to the formation of Reull Vallis (Ivanov and others, 2005; Kostama and others, 2007; Mest and Crown, 2010).

Reull Vallis

Reull Vallis (fig. 1), ~1,100 km long, displays complex morphology indicative of multiple styles and episodes of formation and modification. The Reull Vallis system was previously separated into three morphologically distinct segments (Crown and Mest, 1997; Mest and Crown, 2001); Waikato Vallis includes the former Segment 1 of Reull Vallis and was discussed in a previous section. The upper Reull Valles (formerly Segment 2) is oriented northeast-southwest and winds through Promethei Terra, exhibiting sinuous morphology where it originates within western Eridania Planitia and less sinuous, steep-walled morphology (Mest and Crown, 2001) down-canyon. The lower Reull Vallis (formerly Segment 3) starts at the junction of the upper Reull Vallis with Teviot Vallis (~350 km southwest of the map area), where it alters its course northwestward and terminates near the source basin of Harmakhis Vallis (Mest and Crown, 2001). Along its length, the upper Reull Vallis dissects highland and plains materials of Promethei Terra to its junction with Teviot Vallis (Mest and Crown, 2001, 2003) and channeled plains material where the lower Reull Vallis terminates near the head-canyon of Harmakhis Vallis (Crown and others, 1992; Price, 1998; Mest and Crown, 2001).

The upper Reull Vallis (6–13 km wide, ~350 m deep; fig. 6) displays sinuous morphology and extends for ~220 km through degraded highlands and smooth plains (Mest and others, 1998). Terraces are exposed along both walls of the canyon (figs. 6, 7). Some terraces are believed to be exposed strata and are mapped as smooth plains material (lower member), whereas some terraces appear to be erosional or depositional in nature, possibly representing various stages of flow within Reull Vallis, and these terraces are mapped as scarps. Floor materials in this part of the canyon are incised with a series of braided channels oriented parallel to the canyon walls but also cross from one side of the canyon to the other (fig. 7). These features suggest that at least this part of Reull Vallis is fluvial in nature (Mest and Crown, 2001).

Downstream of the sinuous part of Reull Vallis, in the southwestern part of the map area (fig. 6), a narrow (1.5–2 km wide), shallow (75–100 m deep) canyon downcuts into the main canyon floor (fig. 8) (Mest and others, 1998; Mest and Crown, 2001, 2002, 2003). This section of Reull Vallis is morphologically distinct from the preceding section, displaying steep walls and a relatively flat floor (fig. 9), and is

[2] Previous work by Ivanov and others (2005) and Kostama and others (2007) informally termed this depression the “Morpheos Basin”.

narrower (~6 km) and shallower (~200 m) than the remainder of Reull Vallis to the west (Mest and others, 1998; Mest and Crown, 2001, 2002, 2003). The lack of abundant erosional features (terraces, floor grooves, fluvial channels incised in floor material, streamlined islands) here and in the lower part of Reull Vallis (to the west) suggests subsurface drainage and collapse of plains materials was likely a more dominant process in the formation of these parts of Reull Vallis than fluvial erosion or, at least, dominated the most recent stages of activity, removing indicators of an earlier fluvial phase (Crown and others, 2005).

Channels

Highlands and plains in the region are incised with channels that either occur as single units or join together to form small, poorly developed valley networks. Channels tend to occur in low-lying, low-slope (<2°) areas of crater ejecta and plains materials. Most features are single channels that are less than 1 km wide and several tens to hundreds of kilometers in length. Some channels merge to form networks consisting generally of one to three tributaries, but some have up to a dozen. Channels throughout this region have two basic morphologic types. The first type, which includes most of the channels observed in the map area and the longest features, is shallow, flat-floored, and sinuous in planform (fig. 10). Some of these channels display braided morphology at one or more locations along their length, suggesting unconfined and (or) sediment-loaded flow (Leopold and Wolman, 1957; Schumm and Kahn, 1972; Wohl, 2000). The second type (c in fig. 7) is V-shaped in cross section and deeply incised relative to the narrow valley widths, tends to form short theater-headed valleys, and is found primarily along the sinuous uppermost part of Reull Vallis that is incised within ejecta material from crater Greg. Although some sinuous channels intersect Reull Vallis, it is not clear whether they predate or postdate Reull Vallis, whereas the V-shaped channels display a deeply incised notch in the walls of Reull Vallis, providing clear cross-cutting relations.

Gullies

Gullies are found throughout the southern part of the map area and are incised in the walls of many impact craters and along the slopes of massifs of mountainous material (Berman and others, 2009). The gullies display typical morphologies as described by Malin and Edgett (2000). These gullies generally head within alcoves located just below the crater rim crest or peak of the massif and extend to the base of the slope. They are not deeply incised and some display a fan of material at their termination. Most gullies appear to be incised in the regional mid-latitude mantle (Mustard and others, 2001; Milliken and others, 2003) that superposes most surfaces in the southern part of the map area.

Structural Features

The most abundant and most obvious features in the map area that provide evidence for deformation of surface materials are wrinkle ridges and ridge rings. Formation of wrinkle ridges is generally attributed to folding and (or) thrust faulting resulting from compressional stresses either within the lithosphere or confined within the deforming unit (Lucchitta 1976, 1977; Chicarro and others, 1985; Plescia and Golombek, 1986; Sharpton and Head, 1988; Watters, 1988, 1991, 1993; Golombek and others, 1991; Zuber, 1995; Goudy and Gregg, 2001, 2002; Goudy and Schultz, 2003; Neel and Mueller, 2007). Ridge rings are circular wrinkle ridge-like structures believed to delineate buried craters; it has been suggested that the overlying unit underwent subsidence resulting in compressional stresses over the buried crater rim (Bryan, 1973; Chicarro and others, 1985).

Wrinkle ridges form rings and linear features that consist of a broad arching rise (to 10 km wide and 100 m high) topped with a narrow (~1.5 km wide) crenulated ridge that zigzags from one side of the rise to the other (figs. 2, 4). Regionally, and within the map area, two dominant ridge trends are observed (figs. 1, 2)—northeast-southwest (Hellas radial) and northwest-southeast (Hellas concentric)—indicating the stress regime shifted over time (King, 1978; Watters and Chadwick, 1989; Porter and others, 1991). Most ridges oriented northwest-southeast display the broad rise and narrow crenulated ridge, whereas many ridges oriented northeast-southwest display only the crenulated ridge without the significant presence of the broad rise. Wrinkle ridges are found primarily within the ridged and etched plains materials in the map area, but the highest density of ridges is observed within ridged plains material. Ridges throughout the map area display pristine through degraded morphologies, and, overall, the morphologies do not follow a specific trend. Most of the degraded ridges are found adjacent to and on the floor of Waikato Vallis, within a zone of ridged plains extending from Waikato Vallis to the western edge of the map area and bounded by the ejecta deposits of craters Fitzroy, Avarua, Dowa, and Pál and within the etched plains found on the floor of Eridania Planitia (fig. 2). Based on their locations relative to features believed to have formed, or been modified by, fluvial processes, degradation of ridges may also be due in large part to fluvial processes, but some erosion may be eolian. In addition, some ridges in the smooth and etched plains may be buried, thereby subduing their characteristic morphology.

Cross-cutting and superposition relations suggest wrinkle-ridge formation in the map area occurred after plains emplacement and prior to formation of Waikato and Reull Valles. Several lines of evidence can be used to constrain the timing of wrinkle-ridge formation within the map area. First, the channel incised within the northern depression of Waikato Vallis cuts through several ridges, and ridges exposed on the floor of

Waikato Vallis are notched and do not display the characteristic morphology observed in the ridges as they continue into the adjacent plains. Second, secondary craters and ejecta from the Hesperian-aged craters Dowa and Pál in the north and Greg in the south parts of the map area superpose wrinkle ridges formed within the ridged plains material and etched plains material, respectively. Third, ridges observed within the smooth and etched plains display knobby and pitted textures found throughout the plains, suggesting a regional unit may have been emplaced whose deposition is indifferent to topography, such as the mid-latitude mantle material that is believed to consist of ice-rich sediments deposited via airfall (Mustard and others, 2001; Milliken and others, 2003). In the map area as a whole, ridge-forming deformation may have begun as early as the Early Hesperian Epoch and likely ceased by the mid-Hesperian.

Crater Counting Methodology

Relative ages for the geologic units in MTM –30247, –35247, and –40247 quadrangles were determined by the number and size distribution of superposed impact craters for each geologic unit (Tanaka, 1986; Werner and Tanaka, 2011), as well as by the principles of relative dating. Unit contacts were digitized in ArcGIS on a THEMIS daytime IR mosaic (~230 m/pixel); unit areas were calculated in ArcGIS from the resulting unit polygons. Individual craters were identified on the THEMIS daytime IR base, as well as CTX, THEMIS VIS, and MOC NAC images, for each unit and their diameters were measured and recorded in ArcGIS. Due to near complete coverage of the map area by these high-resolution image datasets, craters ≥0.5 km in diameter were counted; however, given the complex history of erosion, deposition, remobilization, and mantling that could remove a large number of small-diameter craters within primary geologic units, age determinations are based on crater size-frequency distribution data for diameters greater than 1 km. Table 1 summarizes the crater size-frequency distribution data for N(1), N(2), N(5), and N(16) for each geologic unit mapped in MTM –30247, –35247, and –40247 quadrangles. N(1), N(2), N(5), and N(16) represent the cumulative number of craters with diameters >1, 2, 5, and 16 km/10^6 km^2, respectively (crater size-frequency errors = ± $((N^{1/2})/A) \times (106\ k^2)$). The N(1), N(2), N(5), and N(16) data were then plotted for each unit; these data, combined with observations of superposition, cross-cutting, and embayment relations, were used to determine the appropriate time-stratigraphic series for each unit.

Stratigraphy

Relative ages of the geologic units mapped in MTM –30247, –35247, and –40247 quadrangles were determined using crater size-frequency distributions (table 1) in combination with observed stratigraphic relations (table 2). With few exceptions, crater size-frequency distributions show relative ages that tend to be consistent with previous studies (Greeley and Guest, 1987; Crown and others, 1992; Tanaka and Leonard, 1995).

Highland Materials

Highland terrains contain the oldest materials exposed in the area, including mountainous material and materials of the basin-rim unit. Mountainous material (unit Nm) forms large, rugged, isolated, or clustered massifs throughout the map area, but most (and the largest) are concentrated in the southern part. Massifs of unit Nm are found within exposures of the equally ancient basin-rim unit or are surrounded by younger impact ejecta, plains materials, or lobate debris aprons. Mountainous material is believed to consist of ancient crustal material uplifted during impact basin formation (Scott and Tanaka, 1986; Greeley and Guest, 1987) and (or) remnants of eroded crater rims.

Along with mountainous material, the basin-rim unit (unit Nh_1) (Greeley and Guest, 1987) forms most of the highland terrain of Promethei Terra (Mest and Crown, 2001, 2002, 2003) and is found within the southern part of the map area. This unit forms continuous exposures of rugged terrain with expanses of smooth and knobby textured surfaces. Exposures of the basin-rim unit are believed to consist of ancient crustal material uplifted during formation of impact basins and craters subsequently modified by fluvial processes and mass wasting.

In THEMIS day IR and Viking Orbiter images, the highland terrains appear mountainous and rugged (fig. 6). However, in high-resolution images (MOC, THEMIS VIS, and CTX), their surfaces appear rounded and their ruggedness is muted, which appears to be due to erosion of these highland materials followed by mantling by a thin but fairly continuous deposit. Images show that this mantle is being removed from the peaks of some of the steepest massifs and transported downslope via slumping and viscous flows (Milliken and others, 2003) to form deposits of debris apron material (unit Ada) (fig. 9) or talus.

Mountainous material and the basin-rim unit are two of the oldest materials exposed in the map area; N(5) and N(16) crater size-frequency distributions indicate Noachian ages. The range in age for these units is due to (1) their small areas of exposure and (2) burial of small- and medium-diameter craters by mantling material. Based on crater size-frequency distribution statistics (N(5) and N(16)) and superposition relations, mountainous material and the basin-rim unit are most likely Early to Middle Noachian in age.

Plains Materials

Several plains units are mapped, including ridged (upper and lower members), smooth (upper and lower members), etched, and mottled plains materials. Combined, exposed plains materials occupy almost half (49%, ~111,000 km^2) of the total map area; inclusion of the areas of the ejecta blankets that likely superpose large expanses of plains suggests plains materials could cover more than 75 percent (~177,000 km^2) of the total map area.

Most of the map area is located within Hesperia Planum, which contains one of the largest exposures of ridged plains material on Mars (Greeley and Guest, 1987). In this study, ridged plains material, upper member (unit HNpru), covers most of MTMs –30247 and –35247 and likely extends under much of the impact crater materials that superpose the northern part of the map area. Here, unit HNpru is characterized by a high density of wrinkle ridges and ridge rings.

The ridged plains material (upper member) appears mottled at all resolutions displaying large areas of low and high albedo surfaces (figs. 3, 4). In THEMIS day IR images, most inter-ridge areas display relatively smooth and featureless surfaces except for the presence of low-relief scarps and small sinuous channels. CTX and THEMIS VIS images show that inter-ridge areas contain dune features, accumulations of smooth materials in low areas, and small knobs adjacent to some ridges. Some areas within the deposit, especially near Waikato Vallis and within the zone of degraded wrinkle ridges, contain numerous sinuous, and in some cases braided, channels, scarp-bounded mesas, and long (hundreds of kilometers) arcuate scarps that are interpreted to be fluvial in origin (Mest and Crown, 2001).

Previous studies have suggested the ridged plains material of Hesperia Planum was emplaced as flood lavas that filled low-lying regions of the highlands (Potter, 1976; King, 1978; Greeley and Spudis, 1981; Scott and Tanaka, 1986; Greeley and Guest, 1987). However, in this study area, no obvious volcanic features (vents, rilles, flow fronts) are visible, despite the recent abundance of high-resolution images. Narrow sinuous valleys with adjacent dark deposits are found throughout the plains, including within the northern part of this map area, but subsequent modification obscures the precise origin for many of these features. The sinuous nature of many valleys suggests they could be rilles or lava channels, and the dark deposits could be volcanic material. However, numerous other valleys incised in ridged plains material suggest these features could also be fluvial channels with adjacent floodplain deposits. The presence of these fluvial zones, as well as the eolian-dominated inter-ridge areas, suggests unit HNpru has been heavily modified by processes subsequent to its emplacement. Here, we interpret the ridged plains to consist of layered sedimentary and (or) volcanic material, large areas of which have undergone subsequent fluvial and eolian modification that resulted in the mottled appearance of this unit. In addition, chains and clusters of secondary craters, likely originating from craters Dowa and Pál, are found in the central part of the map area within ridged plains material (fig. 3). The ejecta deposits from these two craters (described in more detail below) have also been highly modified, but a thin mantle of these ejecta deposits may be present, contributing to the mottled appearance of this part of the ridged plains material (upper member).

The ridged plains material of Hesperia Planum has been used as the basal referent of the Hesperian System (Tanaka, 1986). However, since the original mapping of these plains (Potter, 1976; King, 1978; Scott and Carr, 1978; Greeley and Guest, 1987), significant improvements in data (such as acquisition of higher-resolution image, spectral, and topographic datasets) have resulted in reclassification of large areas of the Hesperia Planum ridged plains as materials unrelated to flood-basalt-type eruptions (Gregg and Crown, 2005, 2007; Crown and others, 2007). For example, the extent of Tyrrhenus Mons volcanic materials has been reevaluated resulting in a significantly larger area classified as Tyrrhenus Mons shield, flank, and flank flow materials rather than ridged plains material (Porter and others, 1991; Crown and others, 1992; Gregg and others, 1998; Gregg and Crown, 2009; Williams and others, 2008). Also, some areas within Hesperia Planum contain the characteristic wrinkle ridges but are generally less dense than the characteristic ridged plains material and (or) the ridges have been greatly modified; areas of ridged plains material within the south-central part of Hesperia Planum have been remapped as "smooth" and "dissected" plains (Mest and Crown, 2001, 2002, 2003). Lastly, portions of ridged plains material within its southern zone have been subjected to significant amounts of erosion by fluvial processes and (or) burial by eolian and mid-latitude mantling materials.

These subdivisions of Hesperia Planum have ages ranging from Noachian for parts of Tyrrhenus Mons to Amazonian for the Tyrrhenus Mons flank lava flow field. Interestingly, the parts of Hesperia Planum still considered to be ridged plains material show Early Hesperian ages, as defined originally for Hesperia Planum as a whole (Potter, 1976; King, 1978; Scott and Carr, 1978; Greeley and Guest, 1987). Crater size-frequency distribution statistics for the area of ridged plains material (upper member) mapped in this study, combined with superposition relations with ejecta from craters Dowa and Pál, suggest Late Noachian (N(16)) to Early Hesperian (N(2) and N(5)) ages.

Ridged plains material, lower member (unit HNprl), has limited exposure along much of the canyon of Waikato Vallis and forms chaotic clusters of irregularly shaped flat-topped polygons and knobs within the canyon (fig. 4*A*). Most surfaces of unit HNprl are smooth and appear to have similar to slightly higher albedo than the upper member of ridged plains material, and some areas are also mottled in appearance. Other areas display surface textures that are more irregular; these areas tend to be incised with narrow, sinuous valleys that are likely fluvial in nature. Exposures of unit HNprl are typically topographically lower than unit HNpru. The location and appearance of unit HNprl suggests some exposures consist of stratigraphically lower materials exposed during formation of Waikato Vallis. Other exposures may consist of unit HNpru that has undergone collapse and subsequent erosion by fluvial processes. Mottling within the plains is caused by a mantle of eolian and (or) fluvial sediments. Given the nature of Waikato Vallis, as with the source areas of other Martian outflow channels, chaotic areas are interpreted to have formed by collapse of plains materials. Irregular textures within some exposures of unit HNprl reveal these areas are incised with sinuous channels and contain streamlined bedforms, suggesting fluvial modification, likely during vallis formation.

Crater size-frequency distribution statistics for unit HNprl show ages of Early Noachian to Early Hesperian. This unit displays limited extent, but it is superposed by the ejecta of several fresh small-diameter craters. Based on our interpretation of unit HNprl—exposed and (or) collapsed and eroded plains material—we indicate a Late Noachian to Early Hesperian age for the lower member of the ridged plains material.

Smooth plains material consists of an upper member (unit HNpsu) and a lower member (unit HNpsl). Within the map area, the upper member is found primarily adjacent to upper Reull Vallis (figs. 6–8), where it heads within the low-lying plains of Eridania Planitia. Previous mapping of central Reull Vallis to the west of the current study area showed smooth plains material forms much of the plains extending from the canyon of Reull Vallis to the highlands (Mest and Crown, 2001, 2002, 2003). The lower member of the smooth plains material is more limited in exposure, forms the lower wall/lower terraces along much of the length of the uppermost part of Reull Vallis, and is stratigraphically lower than the upper member (figs. 7–9). In THEMIS day IR images, HNpsu displays smooth, relatively featureless surfaces (fig. 6); however, in CTX and THEMIS VIS images, HNpsu displays low-relief scarps and ridges, small channels, and shallow pits or undulations. The upper member exhibits lobate terminations and appears to embay Noachian highland units (Nh_1 and Nm) and highly degraded crater material (discussed below) where they are in contact. Outcrops of HNpsl display smooth and relatively featureless surfaces and appear lower in albedo than the overlying upper member.

Smooth plains materials, both upper and lower members, are interpreted to consist of sediments deposited (1) within a transient body of water, (2) by erosion of adjacent highlands via valley networks, and (or) (3) via mass wasting (Mest and Crown, 2001, 2002, 2003). Most of the materials that constitute the smooth plains materials likely predate formation of the existing Reull Vallis canyon system and were deposited within a transient body of water or by flooding of low-lying regions bounded by the adjacent highlands; a network of transient paleolakes may have extended eastward and been connected with Eridania Planitia (Ivanov and others, 2005; Kostama and others, 2007). The outflow event that formed the uppermost part of Reull Vallis eroded through the upper member of the smooth plains and exposed the lower member, now preserved as terraces along this part of the canyon (fig. 7). Some areas within the upper member could postdate formation of Reull Vallis, consisting of sediments eroded from the adjacent highlands and transported to the plains via valley networks and (or), more recently, as a result of mass wasting of volatile-rich debris from highland massifs. Channels and low-relief scarps found within HNpsu are believed to be fluvial in nature, resulting from drainage of the fluvial event that in part formed Reull Vallis. Shallow pits preserved within HNpsu could have formed by sublimation of volatiles within the plains and subsequent collapse of sediments and (or) could be craters modified by the wind and (or) water.

Crater size-frequency distributions for both members are similar, showing large uncertainties in formation age with younger ages for the lower member because of its limited exposure and exhumed nature and therefore lack of fresh superposed impact craters. Previous mapping by Mest and Crown (2001) showed the smooth plains material was Early Hesperian in age. However, the extent of this unit has since been reduced because of the ability to use higher resolution images to identify ejecta deposits from several of the local large (>50 km in diameter) impact craters, such as craters Greg, Fitzroy, and Avarua, that superpose these plains. We designate ages of Late Noachian to Early Hesperian for the upper and lower members of the smooth plains.

Etched plains material (unit Npe) forms the surface of the topographically low area of Eridania Planitia. The unit extends from the head of Reull Vallis to the east edge of the map area and to the south along the eastern margin of crater Greg. In THEMIS day IR images, unit Npe displays a fairly constant moderate albedo in the northern part of the deposit but is mottled with darker and lighter tones along the east edge of the map area (fig. 6). The northern part of the deposit displays fine-scale knobs and pits. This texture also superposes wrinkle ridges, which display degraded morphologies along their broad rises but fairly sharp unmodified crenulated ridges, and the peaks of small massifs of unit Nm. Two areas within the etched plains material display larger knobs that appear to superpose the plains and wrinkle ridges east of crater Greg and along the northern Npe /HNpsu contact. At these locations it appears that the ejecta from Greg and the smooth plains material grade into zones of knobs (fig. 11*A*). The mottled area of the etched plains material displays surface textures consisting of elongated knobs and pits with a general northeast-southwest orientation (fig. 11*B*). Here, the mottled appearance is due to eolian removal of dark material to expose underlying bright material; the lower albedo (relative to the overall moderate albedo of unit Npe to the north) could be due to concentration of eroded and redistributed material within this part of the plains. Eolian modification of the plains is supported by the presence of an abundance of dust-devil tracks throughout the southern part of unit Npe. Several sinuous, flat-floored, braided valleys are found in the southernmost part of unit Npe, suggesting fluvial processes also modified portions of the plains. Ejecta from several large craters superpose the etched plains material, including crater Greg and unnamed 34- and 20-km-diameter craters along the etched plains material's northeastern and southern contacts, respectively.

The etched plains material is interpreted to be sedimentary in nature, emplaced (1) as lacustrine sediments, (2) from fluvial erosion of the surrounding plains and highlands, and (or) (3) as a wind-blown deposit. Lacustrine sediments suggest that water and sediment released from Waikato Vallis could have been stored within a temporary lake in Eridania Planitia until the lake breached its divide (in the area of crater Lipik) to contribute to Reull Vallis. Ivanov and others (2005) and Kostama and others (2007) suggest a lake level as high as the 650 m contour; however, based on the volume of Waikato Valles, Capitoli and Mest (2010a,b) estimated that a lake in Eridania Planitia likely did not extend above the 450 m contour. The presence of etched plains material on the broad rises of wrinkle ridges and peaks of massifs of mountainous material, as well as on the low-lying plains, suggests a lack of direct topographic control that would be expected in a lake basin and is more consistent with a wind-blown deposit. If deposited in a lake, the depth of water required to submerge knobs and ridges would have extended to the 1,000 m contour, which is significantly greater than estimates by Capitoli and Mest (2010a,b), as well as Ivanov and others (2005) and Kostama and others (2007), and far exceeds the volume of water that appears to have been released from Waikato Vallis. Regardless of its origin, the materials composing the etched plains material appear to be easily eroded by the wind to form the characteristic knob-and-pit texture and yardang-like features. The large knobs just east of crater Greg and along the unit HNpsu/Npe contact are believed to consist of remnants of ejecta from crater Greg and unit HNpsu, respectively. Here, ejecta could have been deposited within a temporary lake located within Eridania Planitia, which drained, thereby exposing the ejecta to enhanced erosion and eolian modification. Numerous chains of degraded secondary craters, believed to have originated from the crater Greg impact event, are also found within unit Npe, supporting the ejecta origin for these large knobs. Sinuous valleys in the southern part of the deposit indicate erosion of plains materials by fluvial processes. Alternatively, the presence of degraded wrinkle ridges and ridge rings within the plains suggests that the etched plains material could consist of a thin mantle of eolian-derived sediments superposing ridged plains material (upper member), and the presence of knobs extending from the upper member of the smooth plains material suggests that portions of these plains may consist of a thin mantle of the lower member of the smooth plains material superposing ridged plains material (upper member).

From crater size-frequency distribution statistics (table 1), etched plains material shows Noachian ages at larger crater sizes (N(5) and N(16)) and a Late Hesperian or younger age at smaller crater sizes (N(2)). Superposition relations with ejecta deposits from several large impact craters along the edge of the deposit, including crater Greg, which shows an age of Late Noachian to Early Hesperian (discussed below), and the fact that the plains superpose wrinkle ridges and unit Nm massifs suggest that etched plains material is Late Noachian in age.

The mottled plains material (unit Npm) fills low-lying areas around highland massifs and degraded craters in the southern part of the map area (fig. 12*A*) and embays these highland units where they are in contact. The surface of mottled plains material displays broad areas of dark and light (mottled) tones throughout the deposit and contains smooth, knobby, and pitted textures. The western and southern parts of the deposit tend to show overall smooth textures in THEMIS day IR images. Some areas of mottled plains material, specifically those adjacent to the southernmost deposits of ejecta from crater Greg (fig. 12*B*), contain fluvial channels with degraded morphologies suggesting burial and (or) modification by collapse of adjacent plains materials. Mottled plains material along the southeastern edge of the map area displays a knobby texture (fig. 12*C*), with areas that exhibit an arcuate, almost lobate edge. Here, unit Npm consists of mostly small (tens of meters across) knobs surrounded by relatively smooth and pitted surfaces, and the knobs appear isolated from a more continuous deposit. Pitted textures appear to be the result of degradation of smooth areas within the plains by collapse of volatile-rich plains and (or) by eolian modification.

Mottled plains material is likely sedimentary in origin, derived from (1) highland materials transported via valleys and (or) emplaced via mass wasting (Mest and Crown, 2001, 2001, 2003), (2) degraded ejecta from local impact craters, and (or) (3) eolian processes. The plains in the northern part of the deposit are found adjacent to highland terrains containing narrow, degraded valley networks that could have deposited sediments into low areas among highland massifs but whose termini are now obscured by subsequent deposits. Mottled plains material nestled within the highlands in the eastern and southern parts of the deposit are within a zone where debris aprons commonly surround highland massifs (see Pierce and Crown, 2003). Coalesced debris aprons could form these parts of mottled plains material (as suggested by Crown and others, 1992, for a region near Harmakhis Vallis in western Promethei Terra). Several large, highly degraded impact craters, such as the 44-km-diameter crater located at lat 42° S., long 112.6° E., are located in the southern part of the map area, and their ejecta deposits would have covered a large portion of this terrain. The location of the knobby terrain relative to large craters, its similarity to the knobby terrains within etched plains material associated with the ejecta east of crater Greg and the smooth plains material, and the almost lobate-like appearance of several clusters of knobs suggest this part of the deposit could represent impact ejecta emplaced in a lacustrine environment that eroded into remnant knobs. CTX images show that the overall appearance of the surfaces of mottled plains material is similar to the mid-latitude mantle deposit where smooth surfaces grade into smooth knobs isolated by pitted surfaces due to desiccation of volatile-rich airfall deposits.

Crater size-frequency distributions suggest an Early Noachian to Early Hesperian age for mottled plains material. Based on superposition relations with ejecta from crater Greg and N(2) crater statistics, the age of mottled plains material is most likely Late Noachian. However, fluvial and eolian modification of these materials, as well as mantling by airfall deposits, suggests younger activity consistent with constraints from smaller diameter craters (for example, N(2)).

Vallis Materials

The floor of Waikato Vallis contains a deposit that is mapped as Waikato Vallis floor material (unit HNwvf). The deposit extends from the northernmost head of the canyon to the south, where the canyon terminates and has breached the rims of two nested craters. Waikato Vallis floor material displays smooth texture in THEMIS day IR images (fig. 4*A*). However, in high-resolution CTX and MOC images, parts of this deposit, especially within its central to southern extent, display fine-scale knobby and pitted textures (fig. 4*C*). Wrinkle ridges intersect the valley at several locations along the length of Waikato Vallis; these exposed ridges exhibit degraded morphology and are mantled with unit HNwvf. Many ridges exposed on the canyon floor are incised with notches at their topographic crests; the down-canyon side of the ridge contains smooth, high-albedo (relative to overall albedo of unit HNwvf) deposits on the canyon floor that are incised with shallow sinuous channels that initiate at these notches. Similarly, at several locations within unit HNwvf (unrelated to wrinkle ridges) there are smooth, bright deposits that are oriented parallel to the canyon walls and are incised with very shallow sinuous channels.

Waikato Vallis floor material likely consists of sediments eroded from the surrounding ridged plains material and emplaced as water moved through the canyon and eventually receded. The notched ridges, bright patches, and sinuous channels provide evidence for flow within the canyon. These features may be areas where transported sediment accumulated, such as within a bar. The overall fine-scale knobby and pitted texture is likely produced by eolian deflation of sediments. Crater size-frequency distribution statistics show that Waikato Vallis floor materials are Noachian in age; the presence of smaller diameter craters (N(2)) suggest Hesperian-aged resurfacing. Cross-cutting relations between Waikato Vallis and ridged plains materials indicates that unit HNwvf must be younger than both ridged plains and modified ridged plains materials, therefore we report a Late Noachian to Early Hesperian age.

Floor materials found in Reull Vallis display different surfaces within the morphologically distinct upper and lower reaches of the canyon. The upper reach, which is sinuous and displays terraces of the smooth plains (lower member) along its walls, contains materials mapped as older Reull Vallis floor material (unit HRvfo). These deposits transition from etched plains material where the head of Reull Vallis emerges from Eridania Planitia. Upper Reull Vallis floor materials display an overall smooth appearance at all image resolutions (figs. 6, 7). Older Reull Vallis floor material is generally smooth and is incised with narrow sinuous channels. Most channels are oriented parallel to the canyon walls, whereas a few meander from side to side along the canyon floor, and in places the channels are braided. A few channels converge at an ~2-km-wide canyon that downcuts into the main canyon of Reull Vallis (fig. 6). This convergence coincides with the location where the older Reull Vallis floor material ends and the younger Reull Vallis floor material (unit AHRvfy) begins, as well as approximately where the morphology of Reull Vallis changes from wide, sinuous, and terraced to narrow, straight, and steep-walled. Older Reull Vallis floor materials also display low-relief scarps that are oriented parallel to the canyon walls, suggesting layers exposed in the walls and (or) erosional terraces.

Older Reull Vallis floor material likely consists of sediments eroded primarily from upstream, with contributions from the adjacent plains and highlands. The sediments were transported by fluvial processes and deposited on the canyon floor. As the available water receded, these deposits were eroded and redistributed to form braided channels and sediment bars. Older Reull Vallis floor material contains few superposed impact craters ≥1 km in diameter (3 craters) and no craters ≥5 km in diameter. N(2) data show an Early Amazonian age with significant uncertainty. From our assessment of the age of etched plains material (Late Noachian) and the upper member of the smooth plains material (Late Noachian/Early Hesperian), initial incision of Reull Vallis likely occurred in the mid-Hesperian, with most activity ceasing in the Late Hesperian. Overprinting the morphology of these materials is a texture characteristic of the mid-latitude mantling deposit (Mustard and others, 2001). In high-resolution images (HiRISE, CTX, and MOC), this deposit mutes the morphology of many craters and likely obscures many of the small-diameter craters superposed on the pre-mantle floor deposit. Older Reull Vallis floor material displays an ambiguous contact with etched plains material, where this unit begins within the headlands of Reull Vallis. Here, many of the surface textures and characteristic features (fine-scale knobs and pits, small sinuous and braided channels) are observed on both units in CTX images. Difficulty in identification of this contact is compounded by the presence of regional mantling materials on both units, and the exact location of the contact between units Npe and HRvfo may vary within a transitional zone extending several tens of kilometers to the east. From these constraints, we have designated the age of older Reull Vallis floor materials to be Late Hesperian.

The lower reach of the upper segment of Reull Vallis, which displays little sinuosity, a flat floor, and steep walls, contains younger Reull Vallis floor material. This deposit begins within the ~2-km-wide canyon incised within the main canyon of Reull Vallis (fig. 8) and continues west of the map area for several hundreds of kilometers (Mest and Crown, 2001, 2002, 2003). These materials display lineations and chains of elongated pits parallel to the canyon walls that are similar to those seen on most mid-latitude lineated valley-fill deposits (Squyres, 1978, 1979; Squyres and Carr, 1986; Crown and others, 1992, 2006). Early work on lineated valley-fill deposits suggested they formed as interstitial ice/water caused unconsolidated materials to undergo shear as the deposit flowed (Squyres, 1978, 1979; Squyres and Carr, 1986), similar to flow in terrestrial rock glaciers (Wahrhaftig and Cox, 1959). However, recent work, with the help of improved topography and new orbital radar instruments (such as Mars Reconnaissance Orbiter Shallow Radar (SHARAD) and Mars Express Mars Advanced Radar for Subsurface and Ionosphere Sounding (MARSIS)), suggests lineated valley-fill deposits consist of a thin debris layer covering a massive ice core that results in glacial-type movement down-canyon (Head and Marchant, 2009; Head and others, 2010; van Gasselt and others, 2010).

Younger Reull Vallis floor material is believed to consist primarily of unconsolidated sediments, eroded primarily from upstream, but also from the adjacent plains and highlands that were fluvially transported and deposited on the floor of this part of the canyon. A portion of the deposit may consist of debris from the canyon walls emplaced via mass movements similar to debris aprons observed elsewhere in the highlands adjacent to Reull Vallis. Movement of the deposit down-canyon, and thus deformation of the surface of the deposit, was facilitated by interstitial ice/water or burial of a massive ice deposit. The observed lineations and elongated and deformed pits in unit AHRvfy are produced by differential shear of the debris/ice mass as it moved down-canyon (Squyres and Carr, 1986).

Previous analyses, based on crater size-frequency distributions and cross-cutting relations with adjacent plains units, have suggested the lineated floor material along the entire length of this part of Reull Vallis ranges from Late Hesperian to Early Amazonian in age (Greeley and Guest, 1987; Crown and others, 1992; Mest and Crown, 2001, 2002, 2003). In this study, younger Reull Vallis floor material displays only two superposed impact craters ≥500 m in diameter within the map area, and no craters ≥1 km in diameter, which we find is consistent with a Late Hesperian to Middle Amazonian age. Extending the age of AHRvfy into the Middle Amazonian compensates for the inclusion of mass-wasted debris in this deposit as debris aprons (see Surficial Deposits), which we believe were active during this time as well.

Surficial Deposits

Debris apron material (unit Ada) appears to have formed the youngest map unit. Exposures of this unit are found throughout the eastern Hellas region and are observed to border highland massifs, crater rims, and vallis walls (Crown and others, 1992; Crown and Stewart, 1995; Stewart and Crown, 1997; Mest and Crown, 2001; Head and others, 2005). Massif-associated deposits (figs. 8, 12) have uniform or mottled albedo and lobate frontal morphologies and appear to be composed of multiple coalescing lobes. Crater-associated deposits (fig. 13) are relatively small and display mottled surfaces and arcuate to lobate fronts. In high-resolution images, massif- and crater-associated deposits display lineations and elongated pits. Lineations consist largely of ridge-and-furrow features, but some lineations are composed of closely spaced to merging elongated pits that are oriented roughly perpendicular to the proposed direction of flow. Deposits of debris apron material along the walls of Reull Vallis are morphologically different than massif- and crater-associated deposits and some vallis-associated deposits observed farther down-canyon (see Crown and others, 1992; Mest and Crown, 2002, 2003). Vallis-associated deposits (fig. 14) do not extend far from the wall and their fronts are steep and roughly parallel to the canyon wall; they are generally lower in albedo (in THEMIS VIS images) relative to adjacent plains and vallis floor materials, and in CTX and HiRISE images they display grooves perpendicular to the source wall and the areas of the deposits are superposed by or degrade into irregular pitted and knobby surfaces, usually on the deposit close to the source wall and along the base of the deposit front, respectively.

Deposits of debris apron material were interpreted to consist of unconsolidated sediments accumulated at the base of topographically higher terrains via mass wasting of highland massifs, crater rims, and vallis walls. Pits within massif- and crater-associated deposits may be from collapse of volatile-rich debris or degraded impact craters (Pierce and Crown, 2003). Lineations on Martian debris aprons are similar to features observed on terminal moraines on Earth and may indicate sorting of material within the flow (Squyres, 1978, 1979). The overall morphology—lobate terminations, ridge-and-furrow texture, and elongated pits—of massif- and crater-associated debris aprons suggests downslope movement of the deposit. Similar to lineated valley fill, early work on debris aprons suggested mobility of these deposits was likely due to incorporation of water or ice (Squyres and Carr, 1986; Crown and others, 1992, 2006; Tanaka and Leonard, 1995; Mest and Crown, 2001). However, recent work utilizing image, topographic, and radar (SHARAD and MARSIS) data has suggested that these features may be more similar to debris-covered glaciers consisting of a thick (~10 m) ice core covered by a thin layer of rock and sediment (Head and others, 2005; Holt and others, 2008; Head and Marchant, 2009; Morgan and others, 2009; Head and others, 2010; van Gasselt and others, 2010). Vallis-associated deposits in the map area appear more like talus deposits than typical mid-latitude lobate debris aprons. The irregular pitted and knobby texture displayed by parts of this deposit may be related to the mid-latitude mantle deposit that covers most terrains in this map area and is likely mass wasting from the vallis walls, as well as from the debris apron front.

Deposits of debris apron material contain few superposed impact craters on their surfaces (13 craters >500 m in diameter) and they are not areally extensive, resulting in limited age constraints. Except for the impact craters that superpose their surfaces, these deposits superpose all materials on which they occur, including highlands, plains, vallis floor materials, and ancient impact crater deposits. Examination of the crater size-frequency distribution for the debris aprons in this map area shows that diameter bins in the 350–750 m range fit the slopes of the Martian isochrons (Hartmann, 2007) and correspond to Early to Middle Amazonian ages.

It should be noted that, although this material is not mapped, mid-latitude mantling deposits cover nearly all surfaces—highlands massifs, impact crater rims, floors and ejecta blankets, plains, vallis walls and floors, and debris aprons—south of ~30° in the map area and subdues characteristic morphologies. This deposit is not static and has undergone mass wasting from highland massifs, crater rims and walls, and vallis walls forming knobby deposits on the slopes or along the bases of these features and (or) viscous flow features (or lobate flows) along the interior walls of impact crater rims (Milliken and others, 2003), such as craters Greg and Fitzroy (Hartmann and others, 2003; Berman and others, 2009), and it fills alcove-headed channels incised along the interior walls of these craters (Berman and others, 2009). Mustard and others (2001) and Head and others (2003) estimated emplacement of the mid-latitude mantle to be Middle to Late Amazonian in age (~0.880 to 0.235 Ga) (Werner and Tanaka, 2011) with degradation of the mantle to be Late Amazonian (younger than ~400 ka). We can use the age of the mantle to constrain the upper ages of most deposits in the map area.

Crater Materials

Impact craters represent discrete events in the geologic record, and their ejecta deposits can serve as unique stratigraphic markers. Materials associated with impact craters—such as the materials that form their floors, rims, and ejecta blankets—are found throughout the map area and cover a significant portion of the surface (~49%, ~90,000 km^2). Impact craters in this area range from the limits of image resolution to ~70 km in diameter, and many have associated geologic units that have been mapped. Most craters have been designated a general unit name based on their morphology (fresh, moderately degraded, or highly degraded). However, some of the larger craters with extensive ejecta blankets, such as craters Greg, Fiztroy, Avarua, Dowa, and Pál (located just west of the map area), are assigned unique geologic labels and are arranged into assemblages.

Crater floor material (unit AHcf) is found on the floors of most craters in the map area, regardless of preservation state, and was previously mapped as smooth floor material (Greeley and Guest, 1987). In THEMIS day IR images, crater floor material appears smooth and featureless (figs. 6, 11*A*). However, in high-resolution images (MOC, THEMIS VIS, CTX, and HiRISE), these deposits show much detail on their surfaces. The margins of many of the crater floor deposits are lobate where they are in contact with the crater walls, and the edges of some deposits are superposed by debris apron material. Deposits of crater floor material display a variety of albedos and surface textures, including knobby, pitted, stucco-type, brain-like, ridge-crater fill (fig. 15*B*) (Carr and Schaber, 1977; Squyres, 1978, 1979, 1989; Lucchitta, 1984; Squyres and Carr, 1986; Crown and others, 1992), are similar to textures observed in craters throughout the highlands, and suggest flow of volatile-rich material across the crater floor, similar to debris aprons and lineated valley fill. Knobby and pitted textures may indicate eolian erosion of poorly indurated fine-grained materials causing deflation of these surfaces forming pits and (or) knobby remnants. Crater floor materials likely consist of (1) sediments derived from crater rim and wall materials, (2) wind-blown sediments derived from external sources (highlands, plains), and (or) (3) ice-rich airfall sediments forming the mid-latitude mantling deposits, especially in the southern part of the map area.

Few craters greater than 500 m in diameter (29 craters) are superposed on crater floor materials, but crater size-frequency distributions show that this unit ranges in age from Late Noachian to Late Amazonian. Some crater floor material, such as the lineated deposits, do not contain any superposed craters; these particular deposits may be composed of coalescing debris aprons, suggesting they formed during the same time as the debris aprons in this area, and these deposits of crater floor material are likely younger. Post-emplacement modification of many of these deposits could have also erased many small craters. Based on the range of surface morphologies and the potential range of sources for these materials, we designate an age of middle to Late Hesperian to Late Amazonian for crater floor materials.

Crater materials within the map area display various states of preservation, indicating degradation of these materials has been a continuing process throughout the evolution of this region. Well-preserved crater material (unit AHc_3) shows the least amount of degradation and is characterized by pronounced, continuous crater rims that are elevated relative to the surrounding terrain and also by well-defined, continuous ejecta blankets. Many of these craters, especially within the plains (ridged and smooth plains materials) near Reull Vallis and in the southern part of the map area, have ejecta deposits that display single- or double-layer ramparts (Barlow, 2006), suggesting impact into volatile-rich materials (Squyres and others, 1992). Moderately degraded crater material (unit HNc_2) shows moderate amounts of degradation, displays crater rims that exhibit minor relief above the surrounding terrain and may be discontinuous in places, and is characterized by discontinuous and (or) poorly exposed ejecta blankets. Highly degraded crater material (unit HNc_1) shows the most degradation in the map area; discontinuous crater rims exhibit little to no relief above the surrounding terrain and ejecta blankets have either been completely eroded or mantled by younger materials, thereby obscuring all characteristic ejecta morphologies. Many craters of all types (well preserved to highly degraded) appear to have smooth, flat floors, containing crater floor material (unit AHcf).

Well-preserved, and moderately and highly degraded crater materials show generally consistent ages based on crater size-frequency distribution data and superposition relations. In the map area, these ages are designated as Late Hesperian and Amazonian for unit AHc_3, Late Noachian to Late Hesperian for unit HNc_2, and Early Noachian to Early Hesperian for unit HNc_1.

The impact events of craters Greg, Fitzroy, Avarua, Dowa, and Pál (west of map area) significantly influenced the geology of the region by distributing their ejecta materials over the surface, disrupting fluvial processes and peppering adjacent materials with their secondary craters, which makes these large craters stratigraphically significant in the geologic record of this area. The rim and ejecta materials were mapped as assemblages either individually (crater Greg), where their rims and ejecta could be separated from other materials, or combined (craters Fitzroy and Avarua, and Dowa and Pál), where their rim materials could be clearly identified but their ejecta blankets could not be separated.

The Greg assemblage consists of Greg crater material (unit HNGc) and Greg ejecta material (unit HNGe) that compose crater Greg (69.6 km in diameter; lat 38.6° S., long 113.0° E.) (figs. 6, 16*A*). Greg crater materials form the rim and central peak of Greg, which exhibit significant relief above their surrounding materials. All Greg-associated features (central peak, rim, floor) are or were superposed by the ice-rich mid-latitude mantle. The north-facing wall of Greg is dissected by channels that generally head within alcoves located at or near the crater's rim crest (fig. 16*B*); most of these channels tend to be filled with debris that exhibits knobby and chevron textures, suggesting the infilling material flowed down-channel (Hartmann and others, 2003; Berman and others, 2009). These channels appear to be incised in the crater wall material, predating the mantle deposit, which suggests the infilling material likely consists of the ice-rich mantle. The south-facing wall of Greg exhibits ice-rich mantle material that extends approximately halfway up the wall (fig. 16*C*); the deposit is dissected by narrow gullies that originate at the upper edge of the mantle. The south-facing wall, above the level of the dissected mantle, is also superposed by several viscous flow features (vff) (Milliken and others, 2003). The vff are generally composed of one or more moraine-like ridges that originate near the crater rim crest and merge to form lobes that narrow significantly downslope and terminate above the upper edge of the dissected mantle. The surface of the vff displays pits and elongated knobs and lineations oriented parallel to the inferred direction of flow. The mantle between the vff and dissected mantle is degrading into a knobby surface that extends downslope into the gullies, where the surface texture transitions to smooth fill that extends to the termini of the gullies.

Greg ejecta material forms several deposits located in the south-central part of the map area that surround Greg and are separated by ridges of mountainous material and Reull Vallis. Exposures of unit HNGe are generally characterized by smooth to hummocky surfaces, but some areas display etched texture or lineations. In CTX images (fig. 17), etched textures west of Reull Vallis are formed by yardang-like features oriented northwest-southeast (radial to Greg), and lineations found in the deposit north of Greg are oriented radial to Greg and may have resulted from emplacement of the ejecta deposit. Valleys are incised within all areas of the ejecta and display sinuous, shallow, and braided morphologies north and south of the crater and adjacent to Reull Vallis and short, straight, box-like canyons that intersect Reull Vallis west of Greg (fig. 7).

The Fitzroy/Avarua assemblage consists of Fitzroy crater material (unit HNFc), Avarua crater material (HNAc), and Fitzroy/Avarua ejecta material (HNFAe) that compose craters Fitzroy (38.3 km in diameter; lat 35.7° S., long 112.0° E.) and Avarua (47.4 km in diameter; lat 35.9° S., long 109.7° E.) (fig. 18). Fitzroy crater material and Avarua crater material form the rims of these craters, both of which exhibit significant relief above the surrounding terrain, but some areas of their rims are eroded and show minor relief. Fitzroy (fig. 19*A*) displays much of the same interior morphology that is observed in Greg, including a north-facing wall dissected with infilled channels that originate within alcoves at or near the crater rim (fig. 19*B*) and a south-facing wall displaying a dissected (probably ice-rich) mantle along the lower part of the wall, lobate vffs along the upper part of the wall, and degraded (knobby and pitted) mantle along the middle of the wall (fig. 19*C*). Only the eastern rim and part of the floor of Avarua are found in the map area. Although Avarua is similar in size, preservation state, and age to Greg and Fitzroy, the mantle deposit appears more continuous across Avarua and less modified than Greg and Fitzroy. For example, Avarua does not display the interior north-facing channels or south-facing gullies that characterize Greg and Fitzroy, and the vffs along Avarua's south-facing wall show broad lobes along their length rather than tapering to a point (fig. 20). The west-facing wall displays smooth mantle on the rim and blocks along the wall and, similar to those observed in Greg and Fitzroy, the mantle appears to flow downslope and forms deposits exhibiting chevron-like texture between the blocks. One significant difference between Avarua and these other large craters is that an unnamed ~23-km-diameter crater impacted the southern rim of Avarua; ejecta from this crater was emplaced on the rim and wall of Avarua and possibly prevented mobilization of the mantle material via mass wasting.

Fitzroy/Avarua ejecta material forms a nearly continuous deposit that completely surrounds Fitzroy but only contacts Avarua along its east and north walls (in the map area), because of the superposed 23-km-diameter crater on its southern rim. The Fitzroy/Avarua ejecta deposit is characterized by a smooth to irregular surface and lobate edges; areas within the deposit are dissected by sinuous and braided channels that converge at or near Reull Vallis.

The Dowa/Pál assemblage consists of Dowa crater material (unit HDc) and Dowa/Pál ejecta material (HDPe) that compose craters Dowa (41.5 km in diameter; lat 31.7° S., long 110.3° E.) and Pál (78.7 km in diameter; lat 31.3° S., long 108.7° E.) (fig. 21). The rim of Pál is located outside of the map area so its rim materials were not mapped, but image analysis indicates ejecta from Pál is significantly blended with ejecta from Dowa, hence the combined ejecta deposit. Dowa crater material forms the rim of Dowa, which exhibits minor relief above the surrounding terrain, and parts of the rim are discontinuous (fig. 22*A*). Dowa exhibits terraces, resulting from slumping of large blocks of wall material along normal faults, along much of the interior wall; the terraces along the western wall are broad relative to the eastern wall, and all terraces display smooth surfaces, suggesting infilling by eolian or mass-wasted sediments. CTX and THEMIS VIS images show a smooth deposit that mantles most surfaces and has moved downslope in some areas to expose crater wall material (fig. 22*B*), especially (1) along the steeper parts of the wall where a lineated (lineations perpendicular to the wall) deposit forms at the base of the crater wall and (2) within gaps in terrace blocks that are filled with materials exhibiting flow textures.

Dowa/Pál ejecta material forms a continuous deposit that completely surrounds Dowa, and visual inspection of images west of the map area reveals that ejecta surrounds Pál as well. This deposit is characterized by an irregular surface, consisting of smooth areas that degrade into larger areas displaying pitted-and-etched texture, revealing a surface that has been highly modified by eolian processes (fig. 23). This texture is formed partly by yardang-like features and wind-eroded depressions that are oriented northwest-southeast (radial to Pál); here the wind is preferentially eroding along the general ray structure of the ejecta contributed by Pál. This texture is also formed by clusters and chains of secondary craters, likely contributed by both Dowa and Pál, that also exhibit evidence for eolian modification. Secondary craters from both Dowa and Pál, forming chains and clusters, are also observed to extend across the topographic depression that defines the northern collapse zone of Waikato Vallis within the ridged plains, as well as the narrow channel that intersects the main canyon of Waikato Vallis.

Crater size-frequency distribution statistics and superposition relations are used to constrain the ages of the materials associated with craters Greg, Fitzroy, Avarua, Dowa, and Pál. Each of these craters has a similar preservation state and their geologic materials also contain similar numbers and size distributions of superposed impact craters. The secondary craters superposed on the ridged plains and Waikato Vallis that were produced by the Dowa and Pál impacts provide an important constraint on the ages of these features; cross-cutting relations suggest that the Dowa and Pál impact events occurred in the Early Hesperian Epoch following ridged plains emplacement and modification. Crater statistics do not provide good constraints for assigning an age to the Fitzroy/Avarua assemblage; these craters are likely Late Noachian or Early Hesperian craters. Crater Greg clearly predates the formation of Reull Vallis and likely formed in the Late Noachian or Early Hesperian as well.

Geologic History

The geologic history of MTM –30247, –35247, and –40247 quadrangles east of the Hellas basin was determined from analysis of images (THEMIS, MOC, CTX, and HiRISE) and MOLA topographic data. Crater size-frequency distributions and cross-cutting and superposition relations were used to constrain the evolution of the region. The following sequence of geologic events was documented by identification of the various types of geologic materials, analysis of the geomorphic characteristics of those materials, and determination of their apparent stratigraphic relations. Although the following events are organized into specific time-stratigraphic sections, there is likely some overlap of events between sections that is not shown.

Early to Middle Noachian:

- Hellas impact event emplaced ejecta and uplifted blocks within highlands of Promethei Terra, forming mountainous material and basin-rim unit. Exposures occur as isolated knobs and massifs, as well as heavily cratered terrain, which contains remnants of larger crater rims from subsequent impacts (HNc_1)

Late Noachian to Early Hesperian:

- Emplacement of ridged plains material throughout region by sedimentary and (or) volcanic processes
- Majority of wrinkle-ridge formation throughout map area occurs after emplacement of plains
- Collapse and erosion of unit HNpru forms Waikato Vallis; ridged plains material within and adjacent to Waikato Vallis underwent erosion by fluvial processes and forms unit HNprl. Sediments deposited on floor of canyon form unit HNwvf
- Water released from ridged plains material via Waikato Vallis flows south and is confined within Eridania Planitia; rim of crater Lipik, as well as other ancient craters and massifs of units Nm and Nh_1, may have acted as barriers. Sediments deposited in basin form unit Npe
- Mottled plains material (unit Npm) emplaced in south part of map area consists of materials eroded from highland terrains interlayered with ejecta from highly degraded (unit HNc_1) and moderately degraded (unit HNc_2) impact craters
- Emplacement of lower (unit HNpsl) and upper (unit HNpsu) members of smooth plains material in south-central part of map area
- Impact events form craters Greg, Fitzroy, and Avarua. Formation of these craters likely contemporaneous with shallow lake within Eridania Planitia as units HNge and HNfae superpose units HNpsu and Npe. Lobate ejecta suggests incorporation of volatiles; ejecta, rim, and wall materials of craters dissected by channels, suggesting erosion as water drained from these surfaces

middle to Late Hesperian:

- Two large impact events form craters Dowa and Pál within ridged plains material in northern part of map area. Secondary crater fields from craters Dowa and Pál superpose northern depressed area and incised channel of Waikato Vallis and wrinkle ridges
- Lipik rim breached resulting in drainage of Eridania Planitia lake and erosion and downcutting into highland materials and units HNpsu and HNpsl to form Reull Vallis
- Sediments emplaced on floor of Reull Vallis form unit HRvfo, which is subsequently dissected by sinuous and braided channels as drainage receded
- Lower part of upper segment of Reull Vallis modified by collapse of plains, as well as fluvial erosion forming narrow canyon within floor of main canyon

mid-Hesperian to Amazonian:

- Impact craters of all morphologic types eroded; sediments emplaced on crater floors via fluvial erosion, eolian deposition, and (or) mass wasting of crater walls to form deposits of unit AHcf
- Volatile-rich sediments deposited on floor of Reull Vallis (unit AHrvfy) result in subsequent down-canyon movement and shear of deposit
- Impact craters with pristine morphologies form (unit AHc_1)

Early to Middle Amazonian:

- Debris aprons (unit Ada) emplaced along walls of highland massifs, impact craters, and vallis walls via mass wasting

Late Amazonian:

- Volatile-rich sedimentary deposit emplaced (likely via airfall) across mid-latitudes within map area; some areas of deposit, especially on steeper slopes, became disaggregated and flowed down-slope, forming talus deposits along massifs of mountainous material or viscous flow features along walls of large craters

Acknowledgments

The authors would like to thank Tracy Gregg, Sharon Wilson-Purdy, and Ken Tanaka for their thoughtful and helpful reviews. This research was supported by grants from NASA's Planetary Geology and Geophysics Program.

References Cited

Barlow, N.G., 2006, Impact craters in the northern hemisphere of Mars—Layered ejecta and central pit characteristics: Meteoritics & Planetary Science, v. 41, p. 1425–1436.

Berman, D.C., Crown, D.A., Bleamaster, L.F., III, 2009, Degradation of mid-latitude craters on Mars: Icarus, v. 200, p. 77–95.

Bryan, W.B., 1973, Wrinkle ridges as deformed surface crust on ponded mare lava, *in* Proceedings of the Fourth Lunar and Planetary Science Conference, Houston, March 5–8, 1973: Houston, TX, Lunar and Planetary Institute, p. 93–106.

Capitoli, E.J., and S.C. Mest, 2010a, Volumetric analysis of the Reull Vallis fluvial system in the eastern Hellas region of Mars—Investigation into the contributions of water: Geological Society of America, Joint Meeting of the Northeastern and Southeastern Sections Baltimore, MD, abstract 10–21.

Capitoli, E.J., and Mest, S.C., 2010b, Volumetric analysis of the Reull Vallis fluvial system in the eastern Hellas region of Mars—Investigation into the contributions of water: El Paso, TX, First International Conference on Mars Sedimentology and Stratigraphy*,* abstract 6017.

Carr, M.H., and Schaber, G.G., 1977, Martian permafrost features: Journal of Geophysical Research, v. 82, p. 4039–4053.

Chicarro, A.F., Schultz, P.H., and Masson, P., 1985, Global and regional ridge patterns on Mars: Icarus, v. 63, p. 153–174.

Crown, D.A., Berman, D.C., and Gregg, T.K.P., 2007, Geologic diversity and chronology of Hesperia Planum, Mars, *in* Abstracts of papers submitted to the Thirty-eighth Lunar and Planetary Science Conference, Houston, March 12–16, 2007: Houston, TX, Lunar and Planetary Institute, abstract 1169.

Crown, D. A., Bleamaster, L.F., III, and Mest, S.C., 2005, Styles and timing of volatile-driven activity in the eastern Hellas region of Mars: Journal of Geophysical Research, v. 110, E12S22, doi:10.1029/2005JE002496.

Crown, D.A., Chuang, F.C., Berman, D.C., and Miyamoto, H., 2006, Ice-driven degradation styles in the Martian mid-latitudes—Constraints from lobate debris aprons, lineated valley fill, and small flow lobes, *in* Abstracts of papers submitted to the Thirty-seventh Lunar and Planetary Science Conference, Houston, March 13–17, 2006: Houston, TX, Lunar and Planetary Institute, abstract 1861.

Crown, D.A., and Greeley, R., 1993, Volcanic geology of Hadriaca Patera and the eastern Hellas region of Mars: Journal of Geophysical Research, v. 98, p. 3431–3451.

Crown, D.A., and Greeley, R., 2007, Geologic map of MTM –30262 and –30267 quadrangles, Hadriaca Patera region of Mars: U.S. Geological Survey Scientific Investigations Map 3079.

Crown, D.A., and Mest, S.C., 1997, Dao, Harmakhis, and Reull Valles—The role of outflow channels in the degradation of the circum-Hellas highlands of Mars, *in* Abstracts of papers submitted to the Twenty-eighth Lunar and Planetary Science Conference, Houston, March 17–21, 1997: Houston, TX, Lunar and Planetary Institute, p. 269–270.

Crown, D.A., Mest, S.C., and Stewart, K.H., 1997, Degradation of the Martian cratered highlands—The role of circum-Hellas outflow channels and constraints on the timing of volatile-driven activity, *in* Conference on Lower Mars—Geologic and Hydrologic Evolution, Physical and Chemical Environments, and the Implications for Life: Lunar and Planetary Institute Contributions No. 916, p. 22–23.

Crown, D.A., Price, K.H., and Greeley, R., 1992, Geologic evolution of the east rim of the Hellas basin, Mars: Icarus, v. 100, p. 1–25.

Crown, D.A., and Stewart, K.H., 1995, Debris aprons in the eastern Hellas region of Mars, *in* Abstracts of papers submitted to the Twenty-sixth Lunar and Planetary Science Conference, Houston, March 13–17, 1995: Houston, TX, Lunar and Planetary Institute, p. 301–302.

Golombek, M.P., Plescia, J.B., and Franklin, B.J., 1991, Faulting and folding in the formation of planetary wrinkle ridges, *in* Proceedings of the Twenty-first Lunar and Planetary Science Conference, Houston, March 12–16, 1990: Houston, TX, Lunar and Planetary Institute, p. 679–693.

Goudy, C.L., and Gregg, T.K.P., 2001, Possible mechanisms of stress in Hesperia Planum, Mars—Digital analysis of mare-type wrinkle ridges, *in* Abstracts of papers submitted to the Thirty-second Lunar and Planetary Science Conference, Houston, March 12–16, 2001: Houston, TX, Lunar and Planetary Institute, abstract 1393.

Goudy, C.L., and Gregg, T.K.P., 2002, Insight to the evolution of wrinkle ridges in Hesperia Planum, Mars, *in* Abstracts of papers submitted to the Thirty-third Lunar and Planetary Science Conference, Houston, March 11–15, 2002: Houston, TX, Lunar and Planetary Institute, abstract 1135.

Goudy, C.L., and Schultz, R.A., 2003, Wrinkle ridges in Hesperia Planum and the stress state in the eastern hemisphere of Mars, *in* Abstracts of papers submitted to the Thirty-fourth Lunar and Planetary Science Conference, Houston, March 17–21, 2003: Houston, TX, Lunar and Planetary Institute, abstract 1475.

Greeley, R., and Crown, D.A., 1990, Volcanic geology of Tyrrhena Patera, Mars: Journal of Geophysical Research, v. 95, p. 7133–7149.

Greeley, R., and Guest, J.E., 1987, Geologic map of the eastern equatorial region of Mars: U.S. Geological Survey Miscellaneous Investigations Series Map I–1802–B, scale 1:15,000,000.

Greeley, R., and Spudis, P.D., 1981, Volcanism on Mars: Reviews in Geophysics, v. 19, p. 13–41.

Gregg, T.K.P., and Crown, D.A., 2005, What is Hesperia Planum, Mars? An examination of multiple working hypotheses, *in* Abstracts of papers submitted to the Thirty-sixth Lunar and Planetary Science Conference, Houston, March 14–18, 2005: Houston, TX, Lunar and Planetary Institute, abstract 1962.

Gregg, T.K.P., and Crown, D.A., 2007, Redefining Hesperia Planum, Mars, through geologic mapping, *in* Abstracts of papers submitted to the Thirty-eighth Lunar and Planetary Science Conference, Houston, March 12–16, 2007: Houston, TX, Lunar and Planetary Institute, abstract 1190.

Gregg, T.K.P., and Crown, D.A., 2009, Mapping Tyrrhena Patera and Hesperia Planum, Mars, *in* Abstracts of the Annual Meeting of Planetary Geologic Mappers, San Antonio, TX: Washington, D.C., National Aeronautics and Space Administration (NASA), Technical Report NASA/CP—2010–216680, p. 27–28.

Gregg, T.K.P., Crown, D.A., and Greeley, R., 1998, Geologic map of the Tyrrhena Patera region of Mars (MTM quadrangle –20252): U.S. Geological Survey Miscellaneous Investigations Series Map I–2556, scale 1:500,000.

Hartmann, W.K., 2007, Martian cratering 9—Toward resolution of the controversy about small craters: Icarus, v. 189, p. 274–278.

Hartmann, W.K., Thorsteinsson, T., and Sigurdsson, F., 2003, Martian hillside gullies and Icelandic analogs: Icarus, v. 162, p. 259–277.

Head, J.W., and Marchant, D.R., 2009, Inventory of ice-related deposits on Mars—Evidence for burial and long-term sequestration of ice in non-polar regions and implications for the water budget and climate evolution, *in* Abstracts of papers submitted to the Fortieth Lunar and Planetary Science Conference, Houston, March 23–27, 2009: Houston, TX, Lunar and Planetary Institute, abstract 1356.

Head, J.W., Marchant, D.R., Dickson, J.L., Kress, A.M., and Baker, D.M., 2010, Northern mid-latitude glaciation in the Late Amazonian period of Mars—Criteria for the recognition of debris-covered glacier and valley glacier landsystem deposits: Earth and Planetary Science Letters, v. 294, p. 306–320.

Head, J.W., Mustard, J.F., Kreslavsky, M., Milliken, R.E., and Marchant, D.R., 2003, Recent ice ages on Mars: Nature, v. 426, p. 797–802.

Head, J.W., Neukum, G., Jaumann, R., 10 others, and The HRSC Co-Investigator Team, 2005, Tropical to mid-latitude snow and ice accumulation, flow, and glaciation on Mars: Nature, v. 434, p. 346–351.

Holt, J.W., Safaeinili, A., Plaut, J.J., and 9 others, 2008, Radar sounding evidence for buried glaciers in the southern mid-latitudes of Mars: Science, v. 322, p. 1235–1238, doi: 10.1126/science.1164246.

Ivanov, M.A., Korteniemi, J., Kostama, V.-P., and 5 others, 2005, Major episodes of the hydrologic history in the region of Hesperia Planum, Mars: Journal of Geophysical Research, v. 110, E12S21, doi:10.1029/2005JE002420.

King, E.A., 1978, Geologic map of the Mare Tyrrhenum quadrangle: U.S. Geological Survey Miscellaneous Investigations Series Map I–910, scale 1:5,000,000.

Kostama, V.-P., Ivanov, M.A., Polit, A.T., and 4 others, 2007, Topographic and morphologic characteristics of Reull Vallis, Mars—Implications for the history of the Reull Vallis fluvial system: Journal of Geophysical Research, v. 112, E11001, doi:10.1029/2006JE002848.

Leopold, L.B., and Wolman, M.G., 1957, River channel patterns—Braided, meandering, and straight: U.S. Geological Survey Professional Paper 282B, p. 39–85.

Lucchitta, B.K, 1976, Mare ridges and related highland scarps—Results of vertical tectonism, *in* Proceedings of the Seventh Lunar and Planetary Science Conference, Houston, March 15–19, 1976: New York, Pergamon Press, p. 2761–2782.

Lucchitta, B.K., 1977, Topography, structure, and mare ridges in southern Mare Imbrium and northern Oceanus Procellarum, *in* Proceedings of the Eighth Lunar and Planetary Science Conference, Houston, March 14–18, 1977: New York, Pergamon Press, p. 2691–2703.

Lucchitta, B.K., 1984, Ice and debris in the fretted terrain: Journal of Geophysical Research, v. 89 (supplement), p. B409–B418.

Malin, M.C., and Edgett, K.S., 2000, Evidence for recent groundwater seepage and surface runoff on Mars: Science, v. 288, p. 2330–2335.

Mars Channel Working Group, 1983, Channels and valleys on Mars: Geological Society of America Bulletin, v. 94, p. 1035–1054.

Maxwell, T.A., and Craddock, R.A., 1995, Age relations of Martian highland drainage basins: Journal of Geophysical Research, v. 100, 11,780–11,780.

Mest, S.C., 2005, Characteristics of impact craters and interior deposits—Analysis of the spatial and temporal distribution of volatiles in the highlands of Mars, *in* Abstracts of papers submitted to the Workshop on the Role of Volatiles and Atmospheres on Martian Impact Craters, Applied Physics Laboratory, Laurel, MD, July 11–14, 2005: Houston, TX, Lunar and Planetary Institute, abstract 3014.

Mest, S.C., 2006, Characteristics of impact crater interior deposits in the southern highlands of Mars, *in* Abstracts of papers submitted to the Thirty-seventh Lunar and Planetary Science Conference, Houston, March 13–17, 2006: Houston, TX, Lunar and Planetary Institute, abstract 2236.

Mest, S.C., 2007, Characteristics of impact crater interior deposits in Noachis Terra, Mars, *in* Abstracts of papers submitted to the Thirty-eighth Lunar and Planetary Science Conference, Houston, March 12–16, 2007: Houston, TX, Lunar and Planetary Institute, abstract 1841.

Mest, S.C., and Crown, D.A., 2001, Geology of the Reull Vallis region, Mars: Icarus, v. 153, p. 89–110.

Mest, S.C., and Crown, D.A., 2002, Geologic map of MTM –40252 and –40257 quadrangles, Reull Vallis region of Mars: U.S. Geological Survey Geologic Investigations Series Map I–2730.

Mest, S.C., and Crown, D.A., 2003, Geologic map of MTM –45252 and –45257 quadrangles, Reull Vallis region of Mars: U.S. Geological Survey Geologic Investigations Series Map I–2763.

Mest, S.C., and Crown, D.A., 2004, Morphologic and morphometric analyses of fluvial systems in the southern highlands of Mars, *in* Abstracts of papers submitted to the Thirty-fifth Lunar and Planetary Science Conference, Houston, March 15–19, 2004: Houston, TX, Lunar and Planetary Institute, abstract 1844.

Mest, S.C., and Crown, D.A., 2005, Impact crater deposits in the Martian highlands, *in* Abstracts of papers submitted to the Thirty-sixth Lunar and Planetary Science Conference, Houston, March 14–18, 2005: Houston, TX, Lunar and Planetary Institute, abstract 1785.

Mest, S.C., and Crown, D.A., 2010, Geologic mapping of the Reull Vallis source area in southern Hesperia Planum, Mars, *in* Abstracts of papers submitted to the Forty-first Lunar and Planetary Science Conference, Houston, March 1–5, 2010: Houston, TX, Lunar and Planetary Institute, abstract 1945.

Mest, S.C., Crown, D.A., Craddock, R.A., and Zimbelman, J.R., 1998, Topographic characteristics of outflow channels in the Martian southern highlands, *in* Abstracts of papers submitted to the Twenty-ninth Lunar and Planetary Science Conference, Houston, March 16–20, 1998: Houston, TX, Lunar and Planetary Institute, abstract #1334 (CD-ROM).

Mest, S.C., Crown, D.A., and Harbert, W., 2010, Watershed modeling in the Terra Tyrrhena region of Mars: Journal of Geophysical Research, v. 115, E09001, doi:10.1029/2009JE003429.

Milliken, R.E., Mustard, J.F., and D.L. Goldsby, 2003, Viscous flow features on the surface of Mars—Observations from high-resolution Mars Orbiter Camera (MOC) images: Journal of Geophysical Research, v. 108, issue E6, no. 5057, doi:10.1029/2002JE002005.

Morgan, G.A., Head, J.W., III, and Marchant, D.R., 2009, Lineated valley fill (LVF) and lobate debris aprons (LDA) in the Deuteronilus Mensae northern dichotomy boundary region, Mars—Constraints on the extent, age and episodicity of Amazonian glacial events: Icarus, v. 202, p. 22–38.

Murray, B.C., Soderblom, L.A., Sharp, R.P., and Cutts, J.A., 1971, The surface of Mars—1. Cratered terrains: Journal of Geophysical Research, v. 76, p. 313–330.

Mustard, J.F., Cooper, C.D., and Rifkin, M.K., 2001, Evidence for recent climate change on Mars from the identification of youthful near-surface ground ice: Nature, v. 412, p. 411–413.

Neel, C.R., and Mueller, K., 2007, Structural analysis of wrinkle-ridge rings on Lunae and Hesperia Planum, Mars—Evidence of buried topography, *in* Abstracts of papers submitted to the Thirty-eighth Lunar and Planetary Science Conference, Houston, March 12–16, 2007: Houston, TX, Lunar and Planetary Institute, abstract 2185.

Pierce, T.L., and Crown, D.A., 2003, Morphologic and topographic analyses of debris aprons in the eastern Hellas region, Mars: Icarus, v. 163, 46–65, doi:10.1016/S0019-1035(03)00046-0.

Plescia, J.B., and Golombek, M.P., 1986, Origin of planetary wrinkle ridges based on the study of terrestrial analogs: Geological Society of America Bulletin, v. 97, p. 1289–1299.

Porter, T.K., Crown, D.A., and Greeley, R., 1991, Timing and formation of wrinkle ridges in the Tyrrhena Patera region of Mars, *in* Abstracts of papers submitted to the Twenty-second Lunar and Planetary Science Conference, Houston, March 18–22, 1991: Houston, TX, Lunar and Planetary Institute, p. 1085–1086.

Potter, D.B., 1976, Geologic map of the Hellas quadrangle of Mars: U.S. Geological Survey Miscellaneous Investigations Series Map I–941, scale 1:5,000,000.

Price, K.H., 1998, Geologic map of the Dao, Harmakhis, and Reull Valles region of Mars: U.S. Geological Survey Miscellaneous Investigations Series Map I–2557, scale 1:1,000,000.

Schubert, G., Solomon, S.C., Turcotte, D.L., Drake, M.J., and Sleep, N.H., 1992, Origin and thermal evolution of Mars, *in* Keiffer, H.H., Jakosky, B.M., Snyder, C.W., and Matthews, M.S., eds., Mars: Tucson, University of Arizona Press, p. 147–183.

Schumm, S., and Kahn, H., 1972, Experimental study of channel patterns: Bulletin of the Geological Society of America, v. 83, p. 1755–1770.

Scott, D.H., and Carr, M.H., 1978, Geologic map of Mars: U.S. Geological Survey Miscellaneous Investigations Series Map I–1083, scale 1:25,000,000.

Scott, D.H., and Tanaka, K.L., 1986, Geologic map of the western equatorial region of Mars: U.S. Geological Survey Miscellaneous Investigations Series Map I–1802–A, scale 1:15,000,000.

Sharpton, V.L., and Head, J.W., 1988, Lunar mare ridges—Analysis of ridge-crater intersections and implications for the tectonic origin of mare ridges, *in* Proceedings of the Eighteenth Lunar and Planetary Science Conference, Houston, March 16–20, 1987: Houston, TX, Lunar and Planetary Institute, p. 307–317.

Squyres, S.W., 1978, Mars fretted terrains, flow of erosional debris: Icarus, v. 34, p. 600–613.

Squyres, S.W., 1979, The distribution of lobate debris aprons and similar flows on Mars: Journal of Geophysical Research, v. 84, p. 8087–8096.

Squyres, S.W., 1989, Water on Mars: Icarus, v. 79, p. 229–288.

Squyres, S.W., and Carr, M.H., 1986, Geomorphic evidence for the distribution of ground ice on Mars: Science, v. 231, p. 249–252.

Squyres, S.W., Clifford, S.M., Kuzmin, R.O., Zimbelman, J.R., and Costard, F.M., 1992, Ice in the Martian regolith, *in* Keiffer, H.H., Jakosky, B.M., Snyder, C.W., and Matthews, M.S., eds., Mars: Tucson, University of Arizona Press, p. 523–554.

Squyres, S.W., Wilhelms, D.E., and Moosman, A.C., 1987, Large-scale volcano-ground ice interactions on Mars: Icarus, v. 70, p. 385–408.

Stewart, K.H., and Crown, D.A., 1997, Geomorphology of debris aprons in the eastern Hellas region of Mars, *in* Abstracts of papers submitted to the Twenty-eighth Lunar and Planetary Science Conference, Houston, March 17–21, 1997: Houston, TX, Lunar and Planetary Institute, p. 1377–1378.

Tanaka, K.L., 1986, The stratigraphy of Mars, *in* Proceedings of the Seventeenth Lunar and Planetary Science Conference, Houston, March 10–14, 1986—Part 1: Journal of Geophysical Research, v. 91 (supplement), p. E139–E158.

Tanaka, K.L., Isbell, N.K., Scott, D.H., Greeley, Ronald, and Guest, J.E., 1988, The resurfacing history of Mars—A synthesis of digitized, Viking-based geology, *in* Proceedings of the Eighteenth Lunar and Planetary Science Conference, Houston, March 16–20, 1987: New York, Cambridge University Press, p. 665–678.

Tanaka, K.L., Kargel, J.S., MacKinnon, D.J., Hare, T.M., and Hoffman, N., 2002, Catastrophic erosion of Hellas basin rim on Mars induced by magmatic intrusion into volatile-rich rocks: Geophysical Research Letters, v. 29, doi:10.1029/2001GL013885.

Tanaka, K.L., and Leonard, G.J., 1995, Geology and landscape evolution of the Hellas region of Mars: Journal of Geophysical Research, v. 100, p. 5407–5432.

Tanaka, K.L., Scott, D.H., and Greeley, Ronald, 1992, Global stratigraphy, *in* Keiffer, H.H., Jakosky, B.M., Snyder, C.W., and Matthews, M.S., eds., Mars: Tucson, University of Arizona Press, p. 345–382.

Van Gasselt, S., Hauber, E., and G. Neukum, 2010, Lineated valley fill at the Martian dichotomy boundary—Nature and history of degradation: Journal of Geophysical Research, v. 115, doi:10.1029/2009JE003336.

Wahrhaftig, C., and Cox, A., 1959, Rock glaciers in the Alaska range: Geological Society of America Bulletin, v. 70, p. 383–486.

Watters, T.R., 1988, Wrinkle-ridge assemblages on the terrestrial planets: Journal of Geophysical Research, v. 93, p. 10,236–10,254.

Watters, T.R., 1991, Origin of periodically spaced wrinkle ridges on the Tharsis plateau of Mars: Journal of Geophysical Research, v. 96, p. 15,599–15,616.

Watters, T.R., 1993, Compressional tectonism on Mars: Journal of Geophysical Research, v. 98, p. 17,049–17,060.

Watters, T.R., and Chadwick, D.J., 1989, Crosscutting periodically spaced first-order ridges in the ridged plains of Hesperia Planum—Another case for a buckling model, *in* Abstracts submitted to the MEVTV Workshop on Tectonic Features on Mars: Houston, TX, Lunar and Planetary Institute, LPI Technical Report No. 89-06, p. 68–70.

Werner, S.C., and Tanaka, K.L., 2011, Redefinition of the crater-density and absolute-age boundaries for the chronostratigraphic system of Mars: Icarus, v. 215, doi:10.1016/j.icarus.2011.07.024.

Williams, D.A., Greeley, R., Werner, S.C., and 4 others, 2008, Tyrrhena Patera—Geologic history derived from Mars Express High Resolution Stereo Camera: Journal of Geophysical Research, v. 113, E11005, doi:10.1029/2008JE003104.

Wohl, E., 2000, Mountain rivers: Washington, D.C., American Geophysical Union, 320 p.

Zuber, M.T., 1995, Wrinkle ridges, reverse faulting, and the depth penetration of lithospheric strain in Lunae Planum: Icarus, v. 114, p. 80–92.

Table 1. Crater size-frequency data and time-stratigraphic determinations for Reull Vallis region of Mars.

[Units listed youngest to oldest as in Description of Map Units. N(1), N(2), N(5), and N(16) represent the cumulative number of craters >1, 2, 5, and 16 km in diameter/10^6 km^2. Error = ± [(N1/2)/A] × 10^6, where A = area in km^2. – = no data; N() not calculated due to no superposing craters. Epoch ranges based upon crater counts using crater-density boundaries determined by Tanaka (1986) and Werner and Tanaka (2011); LA = Late Amazonian; MA = Middle Amazonian; EA = Early Amazonian; LH = Late Hesperian; EH = Early Hesperian; LN = Late Noachian; MN = Middle Noachian; and EN = Early Noachian. Epoch designations are based upon superposition relations and crater counts. See Description of Map Units for names of geologic units and unit subdivisions]

Unit name	Unit label	Area (km^2)	No. ≥1 (km)	No. ≥2 (km)	No. ≥5 (km)	No. ≥16 (km)	N(1)	N(2)	N(5)	N(16)	Epoch range	Epoch designation
Debris apron material	Ada	2,428	1	1	1	0	412±412	412±412	412±412	–	MN–LA	EA–MA
Younger Reull Vallis floor material	AHRvfy	280	0	0	0	0	–	–	–	–	EH–MA	LH–MA
Older Reull Vallis floor material	HRvfo	3,779	3	1	0	0	794±458	265±265	–	–	EH–LA	LH
Waikato Vallis floor material	HNwvf	14,853	52	21	8	3	3,501±486	1,414±309	539±190	202±117	EN-LH	LN–EH
Ridged plains material, upper member	HNpru	131,384	396	110	26	12	3,014±152	837±80	198±39	91±26	MN–LH	LN–EH
Ridged plains material, lower member	HNprl	17,815	58	25	8	3	3,256±428	1,403±281	449±159	168±97	EN–LH	LN–EH
Smooth plains material, upper member	HNpsu	51,780	82	27	14	5	1,584±175	521±100	270±72	97±43	MN–EA	LN–EH
Smooth plains material, lower member	HNpsl	24,788	9	7	3	1	363±121	282±107	121±70	40±40	LN–MA	LN–EH
Mottled plains material	Npm	21,416	62	26	13	2	2,895±368	1,214±238	607±168	93±66	MN–LH	LN
Etched plains material	Npe	35,997	61	22	9	4	1,695±217	611±130	250±83	111±56	MN–EA	LN
Basin–rim unit	Nh1	45,756	90	34	17	8	1,967±207	743±127	372±90	175±62	EN–EA	EN–MN
Mountainous material	Nm	69,875	247	94	43	16	3,535±225	1,345±139	615±94	229±57	EN–EH	EN–MN
Crater floor material	AHcf	5,706	6	1	1	0	1,052±429	175±175	175±175	–	LN–LA	EH–LA
Well-preserved crater material	AHc$_3$	27,117	60	24	6	1	2,334±301	933±191	233±95	39±39	LN–EA	LH–LA
Moderately degraded crater material	HNc$_2$	9,556	23	7	2	0	2,407±502	733±277	209±148	–	LN–EA	LN–LH
Highly degraded crater material	HNc$_1$	25,255	110	30	11	6	4,356±415	1,188±217	436±131	238±97	EN–EH	EN–EH
Ejecta material, Dowa/Pal	HDPe	23,433	69	21	4	1	2,945±355	896±196	171±85	43±43	LN–LH	EH
Crater material, Dowa	HDc	20,347	1	1	0	0	147±85	49±49	–	–	EH–LA	EH
Ejecta material, Greg	HNGe	21,123	51	18	8	1	2,414±338	852±201	379±134	47±47	LN–LH	LN–EH
Crater material, Greg	HNGc	14,603	7	2	1	0	479±182	137±97	68±68	–	EH–MA	LN–EH
Ejecta material, Fitzroy/Avarua	HNFAe	16,848	39	9	1	1	2,315±371	534±178	59±59	59±59	MN–LA	LN–EH
Crater material, Fitzroy	HNFc	13,497	1	0	0	0	74±74	–	–	–	EH–LA	LN–EH
Crater material, Avarua	HNAc	14,276	7	2	1	1	490±185	140±99	70±70	70±70	MN–MA	LN–EH
Crater and ejecta material, Dowa/Pal	HDc + HDPe	23,433	70	22	4	1	2,987±357	939±200	171±85	43±43	LN–LH	EH
Crater and ejecta material, Greg	HNGc + HNGe	21,123	55	18	8	1	2,604±351	852±201	379±134	47±47	MN–EA	LN–EH
Crater and ejecta material, Fitzroy/Avarua	HNFc + HNAc + HNFAe	18,572	40	9	1	1	2,154±341	485±162	54±54	54±54	MN–MA	LN–EH

Table 2. Contact relations of geologic units in Reull Vallis region of Mars.

Unit label	Unit name	Contact relations[1] Younger than	Overlaps with[2]	Older than
Ada	Debris apron material	AHrvfy, Hrvfo, HNwvf, HNpsu, HNpsl, HNprl, Npm, Nh$_1$, Nm, AHcf, HNc$_2$, HNc$_1$, HNge	AHc$_3$	–
AHrvfy	Younger Reull Vallis floor material	HNpsu, HNpsl, Nm	AHrvfo	Ada
Hrvfo	Older Reull Vallis floor material	HNpsu, HNpsl, Nm, HNc$_1$, HNfae	AHrvfy, Npe	Ada, AHc$_3$
HNwvf	Waikato Vallis floor material	HNpru, HNprl, Nm, HNc$_1$	HNc$_2$	Ada, AHc$_3$
HNpru	Ridged plains material, upper member	HNprl, Nm, HNc$_1$	HNprl	HN5f, AHcf, AHc$_3$, HNc$_2$, HNfae, Hdpe
HNprl	Ridged plains material, lower member	Nm, HNc$_1$	HNc$_2$	Ada, HNwvf, HNpru, AHc$_3$
HNpsu	Smooth plains material, upper member	Nm, Nh$_1$, HNc$_1$	HNpsl, HNge, HNfae	Ada, AHrvfy, Hrvfo, Npe, AHc$_3$, HNc$_2$
HNpsl	Smooth plains material, lower member	Nm, Nh$_1$, HNc$_1$	HNpsu, HNge	Ada, AHrvfy, Hrvfo, Npe, AHc$_3$, HNc$_2$
Npm	Mottled plains material	Nh$_1$, Nm, HNc$_1$	Npe	Ada, AHc$_3$, HNc$_2$
Npe	Etched plains material	HNpsu, HNpsl, Nh$_1$, Nm	Hrvfo, Npm, HNge, HNgc	AHc$_3$, HNc$_2$
Nh1	Basin-rim unit	–	Nm, HNc$_1$	Ada, Hrvfo, HNpsu, HNpsl, Npm, Npe, AHcf, AHc$_3$, HNc$_2$, HNgc, HNfae
Nm	Mountainous material	–	Nh$_1$, HNc$_1$	Ada, Hrvfo, HNwvf, HNpsu, HNpsl, HNpru, HNprl, Npm, Npe, AHcf, AHc$_3$, HNc$_2$, HNge, HNgc, HNfae, HNac, Hdpe
AHcf	Crater floor material	HNpru, Nh$_1$, Nm, AHc$_3$, HNc$_2$, HNc$_1$, HNgc, HNfc, Hdpe, Hdc	–	Ada
AHc$_3$	Well-preserved crater material	HNwvf, HNpsu, HNpsl, HNpru, HNprl, Npm, Npe,Nh$_1$, Nm, HNc$_2$, HNc$_1$, HNge, HNgc, HNfae, Hdpe	Ada	AHcf
HNc$_2$	Moderately degraded crater material	HNpsu, HNpsl, HNpru, Npm, Npe, Nh$_1$, Nm, HNge, HNac	HNwvf, HNprl	Ada, AHrvfy, AHcf, AHc$_3$
HNc$_1$	Highly degraded crater material	–	Nh$_1$, Nm	Ada, Hrvfo, HNwvf, HNpsu, HNpsl, HNpru, HNprl, Npm, AHcf, AHc$_3$
Hdpe	Ejecta material, Dowa/Pal	HNpru, Nm	HNc$_2$, Hdc	AHcf, AHc$_3$
Hdc	Crater material, Dowa	–	Hdpe	AHcf
HNge	Ejecta material, Greg	Nh$_1$, Nm, HNc1	HNpsu, HNpsl, Npm, Npe, HNgc	Ada, AHcf, AHc$_3$, HNc$_2$
HNgc	Crater material, Greg	Nh$_1$, Nm	HNpsu, Npe, HNge	AHc$_3$
HNfae	Ejecta material, Fitzroy/Avarua	HNpru, Nh$_1$, Nm, HNc$_1$	HNpsu, HNfc, HNac	Hrvfo, AHc$_3$
HNfc	Crater material, Fitzroy	–	HNfae	AHcf
HNac	Crater material, Avarua	Nm	HNfae	HNc$_2$

[1]Contact relations for units that share in common one or more geologic contacts.

[2]Exhibits one or more locations where contacts between units are topographically or stratigraphically equivalent.